

# Macroscopic Models for Calcium Carbonate Corrosion due to Sulfation. Variation of Diffusion and Volume Expansion.

C. V. NIKOLOPOULOS

*Department of Mathematics, University of the Aegean,  
Karlovasi, 83200, Samos, Greece.  
email: cnikolo@aegean.gr*

*(Received January 2017)*

The subject of the present paper is the derivation and analysis of mathematical models for the formation of a mushy region during calcium carbonate corrosion. More specifically there is emphasis on the variation of the overall diffusion resulting from the changing shape of a single pore due to corrosion process and on the resulting volume expansion of the material as the outcome of the transformation of calcium carbonate to gypsum. These models are derived by averaging, with the use of the multiple scales method applied on microscopic moving - boundary problems. The latter problems describe the transformation of calcium carbonate into gypsum in the microscopic scale. The derived macroscopic models are solved numerically with the use of an implicit in time, finite element method. The results of the simulations for various microstructure geometries in the microscale and a discussion is also presented.

**Key Words:** Sulfation, Concrete Corrosion, Monument Corrosion, Moving Boundary Problems, Perturbation methods.

---

## 1 Introduction

The reaction of hydrogen sulphide or sulphur dioxide with calcium carbonate leads to the creation of gypsum. These reactions are the basic cause for corrosion such as sewer pipes corrosion ([5]), monument's corrosion ([8]), building decay (failures in building fabric caused by corrosion) etc. Mathematical modelling of such a process is useful in order to predict the evolution of the phenomenon as well as its dependence on the physical quantities effecting it. In some cases also this can allow us to choose an optimal strategy to restore or preserve the construction or the monument.

In this framework mathematical models have been developed to describe the sewer pipes corrosion. This was initiated in [5] where a model of Stefan type was presented and analysed. This model was further analysed in later papers as in [6], [9], [10], [20] etc. In the case of monument corrosion again a model of Stefan type was presented in

1 [8], [7]. Additionally a hydrodynamic model for sulfation of calcium carbonate stones  
2 in the form of a reaction diffusion system was presented and analysed extensively in  
3 [1],[2],[3],[12],[13].

4 In the above models a distinct interface separates the corroded and uncorroded parts  
5 of the material. An additional factor that the modelling of these phenomena has to take  
6 into account is that concrete, cement based constructions, as well as a lot of monuments,  
7 for example made of limestone, are porous materials. Then the reaction causing the  
8 corrosion takes place inside the pores of the material. This creates a zone in which  
9 the calcite surrounding the pores is partly corroded and transformed to gypsum that  
10 is we have a kind of mushy region. The later region is formed in the area near the  
11 macroscopic interface which separates the uncorroded region from the partly corroded  
12 one (see Figure(2) point C). Such a model, motivated by the works [17], [18] describing  
13 the solid-liquid phase change, was initially introduced in [22] and extended in [23] for  
14 the case of sewer pipes corrosion. Also for the case of monument corrosion a very similar  
15 model was developed in [24].

16 In the previous models the problem is stated in the microstructure as a typical phase  
17 change problem with a moving boundary. Then applying the process of homogenization  
18 macroscopic equations were derived for the macroscopic scale that is the bulk of the  
19 material. In this work we present an extension of such a modelling approach. The first  
20 additional aspect that it is addressed here is the volume expansion. Transformation of  
21 calcite to gypsum causes volume expansion due to the lower density of gypsum compared  
22 with the calcite. In the previous relevant works this was neglected for simplification.  
23 Another additional aspect addressed here is the fact that it is assumed no diffusion  
24 through out the calcite skeleton. As it will be apparent later in the analysis of the  
25 present model this consideration will lead to the variation of the diffusion coefficient  
26 of the macroscopic equation, which is subject to the shape and the area occupied by  
27 the calcite inside a pore. The modelling approach in the previous works ([22],[23], [24])  
28 is valid if on the contrary it is assumed that we have diffusion everywhere inside the  
29 material even inside the calcite skeleton due to pores of minor size (reaction takes place  
30 only into larger pores). The latter assumption is not a very realistic one but it simplified  
31 the analysis and especially the numerical treatment of the problem.

32 In order to derive a model for the process, initially we need to make some assumptions  
33 about the geometry and the microstructure of the material. A two dimensional approach  
34 is used here. Note that the derivation and analysis is valid for all dimensions, with minor  
35 modifications, but the specific application has only been presented in two dimensions to  
36 avoid at present numerical complications arising in three dimensions. The bulk of the  
37 material is assumed to consist of microscopic identical square cells each one corresponding  
38 to a pore of the material. The detailed description of that is presented in section 2.  
39 Additionally the equations describing the diffusion inside the pores together with the  
40 equations of the moving boundary (outer boundary of the cell and of the shrinking calcite  
41 core) are presented. Next in section 3 the homogenization (averaging) method is applied  
42 to derive the macroscopic equations. In section 4 it is examined how this set of equations  
43 is modified and tackled, via appropriate transformations when this is needed, in order  
44 to treat numerically the problem. Finally in section 5 some numerical simulations are

1 presented together with the adjustment of the model in the sewer pipes corrosion process  
2 as well as in the case of the monument corrosion.

## 3 2 Presentation of The Model

### 4 Description of an Idealized Porous Material

5 Concrete or limestone are porous materials that consist basically of calcium carbonate.  
6 Thus in general we can think of a material under study being a porous one with its  
7 skeleton (the solid part of it), consisting of calcium carbonate. This material under  
8 certain cases may be corroded due to sulfate or sulfur dioxide.

9 We briefly present the basic assumptions used to describe the material which will  
10 enable us to derive a model for its corrosion. Actually this is basically the same setting  
11 as it is described also in [22], [23], [24].

12 We assume that the bulk of the material under study, consists of uniform cells and  
13 that a subdomain of these cells is filled with calcium carbonate while the rest of it is  
14 void. A natural and fairly simple choice is to assume that these cells are of square form.  
15 This will give a two dimensional geometrical description of the microstructure in which  
16 we will focus in this work.

17 This geometrical approach can be justified if we consider inside the material, a calcite  
18 skeleton consisting of long narrow cylindrical bars equispaced and parallel. Then we  
19 may think of a plane intersecting these cylinders transversely and obtain a sequence of  
20 equispaced circular segments corresponding to the calcite parts, while the rest of the plane  
21 corresponds to a net of voids (see Figure 1). Next taking advantage of this symmetrical  
22 setting we consider square cells filling the plane with each one of them containing a  
23 calcite segment centred in it while the rest is void (Figure 2(a)). We may as well assume  
24 that the skeleton bars have different form such as parallelepipedal giving a square or  
25 parallelogram calcite core or elliptic cylinder giving elliptical calcite core etc.

26 Note that our analysis can be carried out similarly if we assume that we have cells  
27 that are line segments and have a one-dimensional geometry ([22]) or alternatively if we  
28 consider cubical cells and three dimensional geometry ([23, 24]). Although in the latter  
29 three-dimensional case the numerical complications are increased and such a case will  
30 not be studied in the present work.

31 It is also worth mentioning that this two dimensional setting for the microstructure  
32 can be further generalized if we consider hexagonal cells or any other polygonal cells  
33 filling the plane. Moreover in each of the above cases we may have an inverted setting,  
34 that is we can take the core of the cells being the void and the rest of the cell filled with  
35 calcite. Therefore we can finally have geometry- dependent variations of the model but  
36 with no essential difference in its basic characteristics and so these considerations will  
37 not be studied further here.

38 Given the above setting about the two dimensional microscale geometry we may as-  
39 sume furthermore that in a local coordinate system a single cell can be defined to occupy  
40 initially the square  $[-1, 1] \times [-1, 1]$ . Additionally the calcite core inside the cell can  
41 be taken to be of symmetrical shape and centred inside the cell. The latter assump-  
42 tion simplifies the analysis that follows but it can be easily dropped without significant  
43 changes.

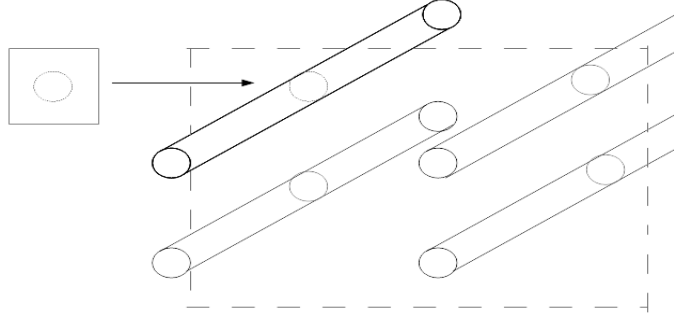


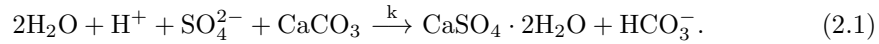
FIGURE 1. Schematic representation of a plane crosssecting parallel bars of a calcium carbonate skeleton. A square on that plane containing the cross section, a circle in this case, centred in it can be considered as one cell in our model.

### 1 The Reactions Causing the Corrosion

2 A material consisting of calcite may be corroded due to the penetration of sulfide or sulfur  
 3 dioxide inside its pores in the presence of water, causing a reaction which transforms  
 4 calcite into gypsum.

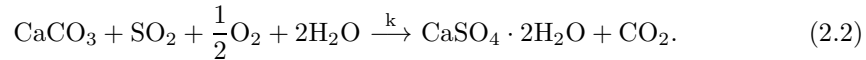
5 We will refer to two basic quite similar reaction processes:

6 The corrosion of concrete by sulfation is the first process. The basic reaction describ-  
 7 ing the fact that  $\text{H}_2\text{SO}_4$  reacts with calcite  $\text{CaCO}_3$  forming gypsum  $\text{CaSO}_4 \cdot 2\text{H}_2\text{O}$  and  
 8 causing concrete corrosion is the following:



9 This is the case in the sewer pipes corrosion (see [5]).

10 In the second case, monument corrosion, we may have penetration of sulfur dioxide  
 11 inside the pores resulting in a similar reaction (see [8], [7]). The basic reaction in this  
 12 case describing the fact that  $\text{SO}_2$  reacts with calcium carbonate  $\text{CaCO}_3$  forming gypsum  
 13  $\text{CaSO}_4 \cdot 2\text{H}_2\text{O}$  and causing the corrosion of the monument, is the following:



14 The model for gypsum formation that is derived in ([22]-[24]) and extended here allows  
 15 gypsum and concrete to coexist at some volume element. This element may be specified  
 16 as one cell as those already described, and having its length side of order similar to the  
 17 radius of a cross-section of a typical pore. Such a model with minor modifications can  
 18 account for both the aforementioned reactions.

19 In the first reaction (concrete corrosion) we have that inside the air and the water,  
 20  $\text{H}_2\text{S}$  is contained and under a chemical reaction in the water film, this is transformed to  
 21  $\text{H}_2\text{SO}_4$ . Next we assume that through the concrete and due to its porosity and the cracks

1 existing in it, there is diffusion (dispersion) of  $\text{SO}_4^{2-}$  which then reacts with the concrete,  
 2 i.e. the calcite, forming gypsum. The reaction takes place initially at the cracks' inner  
 3 surface surrounding the pure solid calcite. Due to the reaction gypsum is formed, having  
 4 larger porosity than that of the concrete and thus new cracks are formed. Then diffusion  
 5 takes place in the gypsum - void, due to cracks, area.

6 Moreover due to the fact that the porosity of the gypsum is larger than that of the  
 7 calcite we have expansion of the cell volume and hence of the overall volume of the  
 8 material. The later is a significant deviation compared with the modelling approach  
 9 adopted in ([22, 23, 24]). In addition, another important difference is that we do not  
 10 allow any kind of diffusion inside the area occupied by the calcite core. Thus the shape  
 11 of the calcite will effect, as it will be apparent later, the diffusion behaviour.

12 The same setting - idealization of the corrosion process - is also assumed for the case  
 13 that we have limestone or calcium carbonate stone corroded by sulfur dioxide.

14 Finally an additional and important assumption that we have to make regarding the  
 15 relevant size of the diffusion and the reaction rate is that the reaction rate at all times is  
 16 large enough so that to have a distinct reaction front ([5], [8]). In the microscopic scale  
 17 the shape of the pore, or equivalently the shape of the calcite core, in the cell will affect  
 18 the diffusion rate. Consequently we assume that, even at its maximum, diffusion is not  
 19 large enough to prevent the formation of a reaction front.

## 20 The Model Equations

21 In the following in order to simplify the presentation we will derive initially a basic  
 22 model keeping the important characteristics of the corrosion process. Then in each case,  
 23 e.g. in sewer pipes corrosion, in monument corrosion or in another similar process, the  
 24 additional aspects or equations can be easily added to describe the actual phenomenon.  
 25 For the above mentioned cases this is done here in section 5.

26 We assume that the material under study occupies a domain, denoted by  $\Omega_M$ , and that  
 27 the pollutant,  $\text{SO}_4^{2-}$  or  $\text{SO}_2$  diffuses inside the pores of it. Its dimensionless concentration  
 28 satisfies the equation

$$\epsilon u_\tau = \Delta u + f, \quad (2.3)$$

29 where  $u$  is the molar concentration of  $\text{SO}_4^{2-}$  ( or of  $\text{SO}_2$  ),  $\epsilon$  is a dimensionless parameter  
 30 (= typical macroscopic length scale squared over diffusion coefficient and typical time  
 31 scale) and  $f$  being a source term modelling the possible production or supply of  $\text{SO}_4^{2-}$  (  
 32 or of  $\text{SO}_2$ ) in the system.

33 Moreover  $u = u(y, \tau)$  and in general  $y \in \Omega_M \subset \mathbb{R}^n$ ,  $n = 1, 2, 3$  depends on the  
 34 macroscopic geometry of the material under study. Also  $\tau$  is the dimensionless time  
 35 variable.

36 The chemical reaction is taking place inside the pores of the material and at the  
 37 outer surface of solid calcium carbonate. This interface will be denoted by  $\Gamma_M$ . This  
 38 interface changes with time, due to the reaction and its motion given by the standard  
 39 kinetic condition expressing the fact that *Speed of the moving Boundary*  $\times$  *Calcium*  
 40 *Carbonate concentration*  $\propto$  *Rate of reaction*. Regarding the rate of reaction, without loss  
 41 of generality, we may assume that it has the form  $R = R(u(y, \tau)) = u(y, \tau)$  as in the case

1 of sewer pipes corrosion ([22, 23]). This law can be modified accordingly to account for a  
 2 different reaction as in the case of monument corrosion (see [24]). Any such modification  
 3 would not change the analysis that follows.

4 Summarizing the above we have that at the boundary  $\Gamma_M$  the kinetic condition ex-  
 5 pressing its motion should be

$$\mathbf{V} = R(u), \quad y \in \Gamma_M, \quad (2.4)$$

6 where  $\mathbf{V}$  is the speed of the moving boundary.

7 Furthermore the flux of  $u$  arriving at the interface is consumed by the chemical reaction  
 8 transforming calcite into gypsum. Thus the boundary condition at the interface of the  
 9 corroded - uncorroded material, given that  $\mathbf{V} = R(y, \tau)$  will be

$$\gamma \frac{\partial u}{\partial n} = \mathbf{V}, \quad y \in \Gamma_M, \quad (2.5)$$

10 where  $n$  is the outward normal vector at a point of the moving boundary  $\Gamma_M$ . This  
 11 condition may be modified to include also transport of the residual reactant due to  
 12 the motion of the boundary. In such a case we would have, in dimensionless form that  
 13  $\gamma \frac{\partial u}{\partial n} = \mathbf{V} + \mathbf{V}u$ . Although the latter at the moment is not included in the model to keep  
 14 things simple.

15 Note also that the dimensionless constant  $\gamma$  after appropriate scaling can be written as  
 16  $\gamma = \gamma_u \frac{1}{\delta}$ , where  $\delta$  is a parameter describing the ratio of the microscopic and macroscopic  
 17 length scales, defined and discussed in detail later.

18 These equations apply in the porous net inside the material in  $\Omega_M$  but since this is  
 19 assumed to be consisting of identical two dimensional cells we may focus on the behaviour  
 20 of the model in just one cell. Recall that such a square cell, say  $\Omega$ , in a local coordinate  
 21 system initially has the form  $\Omega = [-1, 1] \times [-1, 1]$ . Also we denote, at all times, its  
 22 boundary by  $\Gamma_e$ ,  $\partial\Omega = \Gamma_e$ . This cell initially contains pure calcite occupying a subdomain  
 23 of it. This subdomain is of symmetrical shape centred inside the cell.

24 The area occupied by calcite is denoted by  $\Omega_c$  and its boundary  $\partial\Omega_c = \Gamma_c$  separates  
 25 it from the void space. Namely we take the pore, inside the cell, to be specified by the  
 26 boundaries  $\Gamma_e$  and  $\Gamma_c$  and its domain, before the corrosion process starts, is  $\Omega_v = \Omega \setminus \Omega_c$   
 27 (see Figure 2(b)). The area of  $\Omega_v$  should be such that  $\frac{|\Omega_v|}{|\Omega|} = \phi_c$  for  $\phi_c$  being the porosity  
 28 of the porous material. As corrosion evolves and gypsum is formed the boundary  $\Gamma_c$  now  
 29 separates pure calcium carbonate from the gypsum and void parts of the rest of the  
 30 element. We denote the gypsum-void part of the element by  $\Omega_g$  and we have  $\Omega = \Omega_g \cup \Omega_c$   
 31 (see Figure 2(b)). Note that at  $t = 0$ ,  $\Omega_g(0) = \Omega_v$ . This process continues until the  
 32 transformation of the calcium carbonate to gypsum is completed and we have  $\Omega = \Omega_g$ ,  
 33  $\Gamma_c = \emptyset$  (see Figure 2(c)).

34 The set  $\Omega = \Omega(t)$ , varies with time, due to the expansion caused by the reaction  
 35 and this is a significant difference compared with the modelling approach in the works  
 36 [22, 23, 24].

37 Equation (2.3) applies in  $\Omega_g$  and equations (2.4) and (2.5) apply in  $\Gamma_c$ . We also need  
 38 boundary conditions for the boundary  $\Gamma_e$ . Since the material is assumed to be consisting  
 39 of cells of the same form we impose periodic conditions. Denoting the four sides of the

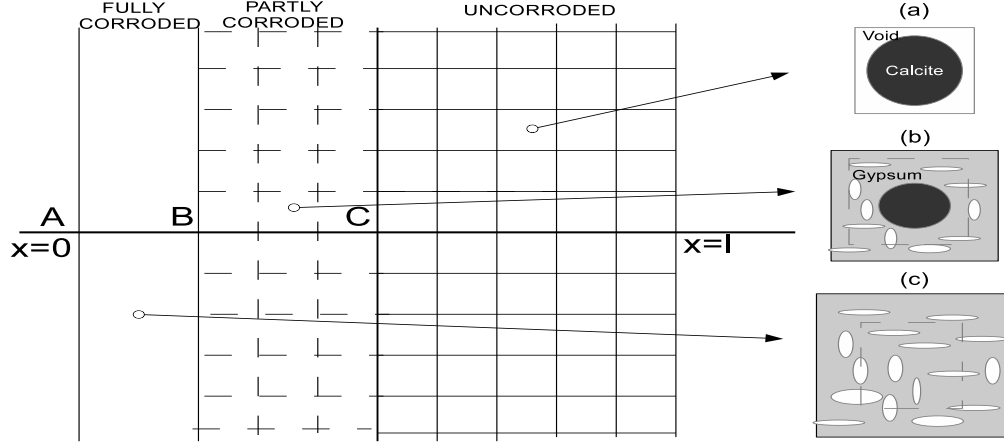


FIGURE 2. Schematic representation of a segment of a calcium carbonate stone under corrosion. In the side cells black color denotes the area of calcium carbonate and grey color denotes the gypsum segments while the rest of the cells (white color) is void space.

1 square cell by  $\Gamma_e^i$ ,  $i = 1, \dots, 4$ , with  $\Gamma_e = \cup_{i=1}^4 \Gamma_e^i$  we write

$$u_{\Gamma_e^1} = u|_{\Gamma_e^3}, \quad u_{\Gamma_e^2} = u|_{\Gamma_e^4} \quad y \in \Gamma_e, \quad (2.6 a)$$

2

$$n \cdot \nabla u|_{\Gamma_e^1} = n \cdot \nabla u|_{\Gamma_e^3}, \quad n \cdot \nabla u|_{\Gamma_e^2} = n \cdot \nabla u|_{\Gamma_e^4} \quad y \in \Gamma_e. \quad (2.6 b)$$

3 Note that these symmetry conditions can be summarized, (see [22], [17]), to obtain

$$n \cdot \nabla u|_{\partial\Omega} = 0 \quad y \in \Gamma_e.$$

4 Additionally the boundary  $\Gamma_e$  is expanding. For an area transformed to gypsum, let  
 5 say  $A_g$  ( $A_g(\tau) = |\Omega_c|(0) - |\Omega_c|(\tau)$ ), we expect an increase of the total cell area of  $\gamma_a A_g$   
 6 where  $\gamma_a$  is a factor corresponding to the expansion resulting from one unit area of  
 7 calcium carbonate transformed to gypsum.

We determine  $\gamma_a$  so that to account during the reaction, for both the changes in densities and the porosity. For  $\rho_c$  and  $\rho_g$  being the values of the real <sup>1</sup> (or solid) densities of calcite and gypsum respectively we have, before the reaction initiates, that a unit mass of calcite occupies volume  $|\Omega_c|(0) = 1/\rho_c$  in a cell of volume  $|\Omega|(0)$ . Thus for  $\phi_c$  being the porosity of the calcite we have  $\phi_c = \frac{|\Omega|(0) - 1/\rho_c}{|\Omega|(0)}$  and  $|\Omega|(0) = \frac{1}{\rho_c(1-\phi_c)}$ . At the end of the process, at time say  $T$ , we have that by a molar unit of calcite a molar unit of gypsum is created (conservation of mass). Therefore the transformed mass of gypsum will occupy volume  $1/(\rho_g \times \rho_m)$ , for  $\rho_m = (\rho_{Mc}/\rho_{Mg})$  where  $\rho_{Mg}$  and  $\rho_{Mc}$  are the molar densities of gypsum and calcite respectively. Thus, for  $\phi_g$  being the porosity of the gypsum,  $\phi_g = \frac{|\Omega|(T) - 1/(\rho_g \rho_m)}{|\Omega|(T)}$  or that  $|\Omega|(T) = \frac{1}{\rho_g \rho_m (1-\phi_g)}$ . In addition at the same

<sup>1</sup> the mass/volume ratio of a porous material; i.e., excluding the pore volume in contrast to bulk density which measures the mass/volume ratio that includes the cavities in a porous material, c.f.[11].

time we should have  $|\Omega|(T) = |\Omega|(0) + \gamma_a |\Omega_c|(0)$ . Therefore we obtain

$$\frac{1}{\rho_g \rho_m (1 - \phi_g)} = \frac{1}{\rho_c (1 - \phi_c)} + \gamma_a \frac{1}{\rho_c},$$

or

$$\gamma_a = \frac{\rho_c}{\rho_g \rho_m (1 - \phi_g)} - \frac{1}{(1 - \phi_c)} = \frac{\rho_c (1 - \phi_c) - \rho_g \rho_m (1 - \phi_g)}{\rho_g \rho_m (1 - \phi_c) (1 - \phi_g)}.$$

1 Note also that  $\gamma_a > 0$ , for  $\rho_c > \rho_g$ ,  $\phi_g > \phi_c$ ,  $\rho_m < 1$  since  $\frac{\rho_c}{\rho_g} > 1 > \rho_m \frac{1 - \phi_g}{1 - \phi_c}$ . The total  
 2 area of the cell at time  $\tau$  will be  $|\Omega|(0) + \gamma_a A_g$ . The latter corresponds to an increase of  
 3 the side of an expanding square cell of magnitude  $\sqrt{|\Omega|(0) + \gamma_a A_g} - \sqrt{|\Omega|(0)}$ . Motivated  
 4 by this we assume that the speed of the outer boundary should be proportional to the  
 5 rate of increase of the above quantity. Namely we have for  $V_e$  the speed of the moving  
 6 boundary  $\Gamma_e$

$$V_e = \frac{\partial}{\partial \tau} \left( \sqrt{|\Omega|(0) + \gamma_a A_g(\tau)} \right). \quad (2.7)$$

7 At this point we should make the remark that considering one - dimensional cells and  
 8 using a similar argument we would have that the speed of the outer cell boundary should  
 9 be proportional to the rate of increase of the inner boundary and have  $V_e = -\gamma_a V$  (c.f.  
 10 [5], [22]) with  $\Gamma_e$  initially being the points  $-1, 1$ .

11 Alternatively for a cubic cell and now for  $V_g = |\Omega_c|(0) - |\Omega_c|(\tau)$  the same argument  
 12 results in taking  $V_e = \frac{\partial}{\partial \tau} \left( \sqrt[3]{|\Omega|(0) + \gamma_a V_g(\tau)} \right)$ .

Moreover we have to note that another, alternative and more simple modelling ap-  
 proach, is to assume that at all times the outer boundary has the form of a square which  
 is expanding. If its side is initially equal to  $\sqrt{|\Omega|(0)} = 2$ , then at time  $\tau$ , it should be,  
 $2(1 + \zeta(\tau))$  with  $(2(1 + \zeta))^2 = 4 + \gamma_a A_g(\tau)$ . Thus the position of the outer boundary can  
 be determined at all times by the following algebraic equation

$$1 + \zeta(\tau) = \sqrt{1 + \frac{1}{4} \gamma_a A_g(\tau)}.$$

13 Although to give more generality in the following analysis we will assume that the position  
 14 of the outer boundary will be given from equation (2.7).

### 3 Homogenization

15  
 16 We next apply the method of homogenization for the model represented by the system  
 17 of equations (2.3),(2.4), (2.5), (2.6) and (2.7). The method of homogenization is a very  
 18 powerfull tool applied here to derive a macroscopic model. This form of homogenization  
 19 ([21]), as well as similar homogenization methods as FE2 modelling ([27]) or distributed  
 20 modelling ([4]) is part of a research area which has been immensely developed during  
 21 the last decades. Moreover this method allow us from the problem in the microscale to  
 22 derive equations in the macroscopic scale. The latter equations will actually describe the  
 23 corrosion process and more specifically the evolution of the mushy (mixed) region which  
 24 is formed. By the term mushy (mixed) region we describe the region that corroded and  
 25 uncorroded parts of the material coexist through out the bulk of it (see [17], [18] and  
 26 [22]-[24]).



1 We consider two spatial scales for the problem: a macroscopic length scale represented  
 2 by the variable  $y$  and a microscopic length scale represented by the variable  $z$ . Let  $l$  be  
 3 a typical macroscopic length scale, and  $d$  the microscopic length scale. The scale  $l$  can  
 4 be taken to be a typical length of the observed corrosion in a time period of interest or  
 5 a length associated with the thickness of material. In addition the microscopic length  
 6 scale  $d$  can be taken to be of order of an average distance between two pores inside the  
 7 material or the average diameter of a pore inside it.

8 Naturally  $d \ll l$  and their ratio is  $\delta = \frac{d}{l} \ll 1$ . More specifically we have that for  $x$   
 9 being the dimensional original distance,  $x = ly$  and  $x = dz$  with  $\delta = \frac{d}{l} \ll 1$ .

10 Moreover the concentration  $u$  is regarded as a function of both dimensionless distances,  
 11  $y$  and  $z$  as well as of time  $\tau$  and  $u = u(y, z, \tau)$ . The multiple scales approach (see [14]) gives  
 12 instead for the spatial derivative  $\nabla_y u$  at the point  $(y, z, t)$  the expression  $\nabla_y u + \frac{1}{\delta} \nabla_z u$ .

13 The boundary  $\Gamma_c$  is assumed to be described by some function  $\mathbf{s} = \mathbf{s}(y, \tau)$  ( $\mathbf{s} = s/l$ )  
 14 for  $s$  the dimensional boundary position. The position of the boundary  $s$  can be rescaled  
 15 with  $d$  and we take  $S = \frac{s}{d}$  ( $= \frac{l}{d} \mathbf{s} = \frac{1}{\delta} \mathbf{s}$ ).

16 Rescaling also with  $d$  the speed of the boundary  $V$ , will give  $V = \delta \mathcal{V}$ , where  $\mathcal{V}$  is the new  
 17 dimensionless variable for the speed (Dimensional boundary speed =  $Vl/t_0 = \mathcal{V}d/t_0$ , or  
 18  $V = \delta \mathcal{V}$ ). This implies that  $\delta \mathcal{V} = R(u)$  on  $\Gamma_c$ .

19 If we denote with  $\mathcal{S}$  the function representing the position of the boundary in the form  
 20  $\mathcal{S}(y, z, \tau) = 0$ , ( $\mathcal{S}(y, z, \tau) = z_2 - \mathcal{S}(y, z_1, \tau) = 0$ ), we have that the rescaled speed of the  
 21 boundary  $\mathcal{V}$ , ([23]) has the form

$$\delta \mathcal{V} = \frac{\partial \mathcal{S}}{\partial \tau} \frac{1}{|\nabla_z \mathcal{S} + \delta \nabla_y \mathcal{S}|}.$$

22 Application of the multiple scales method implies

$$\varepsilon u_\tau = \frac{1}{\delta^2} \nabla_z^2 u + \frac{2}{\delta} \nabla_y \nabla_z u + \nabla_y^2 u + f.$$

23 Regarding the Kinetic condition, (2.4), we have at  $\Gamma_c$ ,

$$\delta \mathcal{V} = \frac{\partial \mathcal{S}}{\partial \tau} \frac{1}{|\nabla_z \mathcal{S} + \delta \nabla_y \mathcal{S}|} = -\gamma_u \frac{1}{\delta^2} n \cdot [\nabla_z u + \delta \nabla_y u],$$

24 as well as, regarding equation (2.5),

$$\gamma_u n \cdot [\nabla_z u + \delta \nabla_y u] + \delta^2 R(u) = 0.$$

25 At the boundary  $\Gamma_e$  similarly we have

$$n \cdot [\nabla_z u + \delta \nabla_y u]_{\Gamma_e^{1,2}} = n \cdot [\nabla_z u + \delta \nabla_y u]_{\Gamma_e^{3,4}},$$

26

$$u_{\Gamma_e^{1,2}} = u_{\Gamma_e^{3,4}}.$$

27 As for  $\Gamma_c$  the position of the boundary  $\Gamma_e$  can be expressed by a function  $\mathcal{Z}(y, z, \tau) = 0$ ,  
 28 with  $\mathcal{Z}(y, z, \tau) = z_2 - \mathcal{Z}(y, z_1, \tau) = 0$ . The rescaled speed of the boundary  $\Gamma_e$ ,  $\mathcal{V}_e$ ,  
 29 ( $\mathcal{V}_e = \delta \mathcal{V}_e$ ) has the form

$$\delta \mathcal{V}_e = \frac{\partial \mathcal{Z}}{\partial \tau} \frac{1}{|\nabla_z \mathcal{Z} + \delta \nabla_y \mathcal{Z}|}.$$

30 In the following we proceed with a formal asymptotic expansion for  $u$ ,  $S$  and  $Z$ .

1 Moreover, for the approximations that follow to be valid, we assume that the shape of  
2 the calcium carbonate core does not wildly fluctuating from cell to cell.

3 The equation for  $u$ , by assuming that  $u \sim u_0 + \delta u_1 + \dots$ ,  $f = f_0 + \delta f_1 + \dots$  takes the  
4 form

$$\begin{aligned} \epsilon u_{0\tau} + \dots &= \frac{1}{\delta^2} \nabla_z^2 u_0 + \frac{2}{\delta} \nabla_z \nabla_y u_0 + \nabla_y^2 u_0 + f_0 \\ &+ \frac{1}{\delta} \nabla_z^2 u_1 + 2 \nabla_z \nabla_y u_1 + \nabla_z^2 u_2 + \dots \end{aligned}$$

5 At the points  $(y, z, \tau)$  of the boundary  $\Gamma_c$ , we have for  $\mathcal{S} = \mathcal{S}_0 + \delta \mathcal{S}_1 + \dots$ , and  
6  $|\nabla_z \mathcal{S} + \delta \nabla_y \mathcal{S}| = |\nabla_z \mathcal{S}_0 + \delta \nabla_y \mathcal{S}_0 + \delta \nabla_z \mathcal{S}_1 + \dots|$ , that

$$\frac{\partial \mathcal{S}_0}{\partial \tau} \frac{1}{|\nabla_z \mathcal{S}_0|} = -\gamma_u n \cdot \left[ \frac{1}{\delta^2} \nabla_z u_0 + \frac{1}{\delta} \nabla_y u_0 + \frac{1}{\delta} \nabla_z u_1 + \nabla_y u_1 + \nabla_z u_2 + \dots \right], \quad (3.2 a)$$

$$R(u_0) + \dots + \gamma_u n \cdot \left[ \frac{1}{\delta^2} \nabla_z u_0 + \frac{1}{\delta} \nabla_y u_0 + \frac{1}{\delta} \nabla_z u_1 + \nabla_y u_1 + \nabla_z u_2 \right] + \dots = 0. \quad (3.2 b)$$

8 Similarly at the points  $(y, z, \tau)$  of the boundary  $\Gamma_e$  we have

$$n \cdot \left[ \frac{1}{\delta^2} \nabla_z u_0 + \frac{1}{\delta} \nabla_y u_0 + \frac{1}{\delta} \nabla_z u_1 + \dots \right]_{\Gamma_e^{1,2}} = n \cdot \left[ \frac{1}{\delta^2} \nabla_z u_0 + \frac{1}{\delta} \nabla_y u_0 + \frac{1}{\delta} \nabla_z u_1 + \dots \right]_{\Gamma_e^{3,4}} \quad (3.3 a)$$

$$[u_0 + \delta u_1 + \delta^2 u_2 + \dots]_{\Gamma_e^{1,2}} = [u_0 + \delta u_1 + \delta^2 u_2 + \dots]_{\Gamma_e^{3,4}}. \quad (3.3 b)$$

11 Additionally regarding its motion we have that the corroded area is

$$12 A_g(\tau) = |\Omega_c|(0) - |\Omega_c|(\tau) = \int_0^1 (S(y, z_1, 0) - S(y, z_1, \tau)) dz_1 \text{ and}$$

$$\frac{\partial \mathcal{Z}_0}{\partial \tau} \frac{1}{|\nabla_z \mathcal{Z}_0|} + \dots = \frac{\partial}{\partial \tau} \left( \sqrt{1 + \frac{1}{4} \gamma_a \int_0^1 (S_0(y, z_1, 0) - S_0(y, z_1, \tau)) dz_1} \right) + \dots \quad (3.4)$$

13 For order  $O(\frac{1}{\delta^2})$  terms we have  $\nabla_z^2 u_0 = 0$ . By the conditions at the moving boundary  $\Gamma_c$ ,  
14 i.e. at  $z = S$  we get  $n \cdot \nabla_z u_0 = 0$ . In addition at the other boundary, the cell boundary  
15  $\Gamma_e$ , we have periodic conditions  $n \cdot \nabla_z u_0|_{\Gamma_e^{1,2}} = n \cdot \nabla_z u_0|_{\Gamma_e^{3,4}}$ ,  $u_0|_{\Gamma_e^{1,2}} = u_0|_{\Gamma_e^{3,4}}$ . By these  
16 equations and the maximum principle we deduce that  $u_0 = u_0(y, \tau)$  in  $\Omega_g$ .

17 For order  $O(\frac{1}{\delta})$  terms we have  $2 \nabla_z \nabla_y u_0 + \nabla_z^2 u_1 = 0 = \nabla_z^2 u_1 = 0$  in  $\Omega_g$ , given  
18 that  $u_0 = u_0(y, \tau)$ . Moreover on  $\Gamma_e$  the periodic conditions  $n \cdot [\nabla_y u_0 + \nabla_z u_1]_{\Gamma_e^{1,2}} =$   
19  $n \cdot [\nabla_y u_0 + \nabla_z u_1]_{\Gamma_e^{3,4}}$ , or  $n \cdot [\nabla_z u_1]_{\Gamma_e^{1,2}} = n \cdot [\nabla_z u_1]_{\Gamma_e^{3,4}}$  and  $u_1|_{\Gamma_e^{1,2}} = u_1|_{\Gamma_e^{3,4}}$  hold. Finally  
20 on  $\Gamma_c$  we obtain similarly  $n \cdot [\nabla_y u_0 + \nabla_z u_1] = 0$  or  $n \cdot [\nabla_z u_1] = -n \cdot [\nabla_y u_0]$ . The latter  
21 condition gives a  $z$  dependence on  $u_1$ ,  $u_1 = u_1(y, z, \tau)$ .

22 In order to control the  $z$ -dependance of  $u_1$  which comes from the fact that its gradient  
23 is proportional to  $n \cdot [\nabla_y u_0]$  at the boundary we define an auxiliary cell problem.

24 On writing  $u_1 = w \cdot \nabla_y u_0$  for  $w = w(z) = (w_1(z), w_2(z))$ , we obtain the following cell  
25 problems

$$\nabla_z^2 w_i = 0, \quad \text{in } \Omega_g, \quad (3.5 a)$$

$$n \cdot \nabla_z w_i = -n_i, \quad \text{on } \Gamma_c, \quad (3.5 b)$$

$$[n \cdot \nabla_z w_i]_{\Gamma_e^{1,2}} = [n \cdot \nabla_z w_i]_{\Gamma_e^{3,4}}, \quad w_i|_{\Gamma_e^{1,2}} = w_i|_{\Gamma_e^{3,4}} \quad \text{on } \Gamma_e, \quad (3.5 c)$$

28 for  $i = 1, 2$  and  $n_i$  the directional cosines of the unit normal  $n = (n_1, n_2)$ . These cell

1 functions actually are describing the effect of the shape, of the area in which diffusion  
2 takes place, to the overall diffusion coefficient.

3 Next for  $O(1)$  terms, we have

$$\varepsilon u_{0\tau} = \nabla_y^2 u_0 + 2\nabla_z \nabla_y u_1 + \nabla_z^2 u_2 + f_0, \quad (3.6)$$

4 while at the the boundary  $\Gamma_c$ ,

$$\frac{\partial \mathcal{S}_0}{\partial \tau} \frac{1}{|\nabla_z \mathcal{S}_0|} = -\gamma_u n \cdot [\nabla_y u_1 + \nabla_z u_2] = R(u_0). \quad (3.7)$$

5 and similarly at the boundary  $\Gamma_e$ , we have

$$n \cdot [\nabla_y u_1 + \nabla_z u_2]_{\Gamma_e^{1,2}} = n \cdot [\nabla_y u_1 + \nabla_z u_2]_{\Gamma_e^{3,4}}, \quad u_2|_{\Gamma_e^{1,2}} = u_2|_{\Gamma_e^{3,4}}, \quad (3.8)$$

6 and

$$\frac{\partial \mathcal{Z}_0}{\partial \tau} \frac{1}{|\nabla_z \mathcal{Z}_0|} = \frac{\partial}{\partial \tau} \left( \sqrt{1 + \frac{1}{4} \gamma_a \int_0^1 (S_0(y, z_1, 0) - S_0(y, z_1, \tau)) dz_1} \right). \quad (3.9)$$

7 We next proceed by averaging the field equation, (3.6), over the whole domain occupied  
8 by the pore-gypsum area, say  $\Omega_g$ . That is we integrate both sides with respect to  $z$  over  
9  $\Omega_g$  to eliminate the  $z$ -dependence from the equations.

$$\int_{\Omega_g} [\varepsilon u_{0\tau} - \nabla_y^2 u_0 - 2\nabla_z \nabla_y u_1 - f_0] dz = \int_{\Omega_g} \nabla_z^2 u_2 dz = \int_{\Gamma_c \cup \Gamma_e} n \cdot \nabla_z u_2 ds, \quad (3.10)$$

10 Note here that

$$\int_{\Omega_g} [2\nabla_z \cdot \nabla_y u_1] dz = \int_{\Omega_g} 2\nabla_z \cdot \nabla_y (w \cdot \nabla_y u_0) dz = \left( 2 \int_{\Omega_g} \nabla_z \cdot w dz \right) \nabla_y^2 u_0,$$

11 and additionally, in view of the relation  $\int_{\Gamma_e} n \cdot \nabla_z \cdot u_2 dz = 0$  and of the second part of  
12 equation (3.7), we have

$$\begin{aligned} \int_{\Gamma_c \cup \Gamma_e} n \cdot \nabla_z u_2 ds &= \int_{\Gamma_c} n \cdot \nabla_z u_2 ds = \int_{\Gamma_c} \left[ -n \cdot \nabla_y u_1 - \frac{1}{\gamma_u} R(u_0) \right] ds \\ &= \int_{\Gamma_c} [-n \cdot \nabla_y (w \cdot \nabla_y u_0)] ds - \frac{1}{\gamma_u} \int_{\Gamma_c} R(u_0) ds \\ &= -\nabla_y^2 u_0 \int_{\Gamma_c} [n \cdot w] ds - \frac{1}{\gamma_u} R(u_0) \int_{\Gamma_c} ds \\ &= -\nabla_y^2 u_0 \left( \int_{\Omega_g} \nabla_z \cdot w dz \right) - \frac{1}{\gamma_u} R(u_0) |\Gamma_c|, \end{aligned}$$

13 for  $|\Gamma_c| = \int_{\Gamma_c} ds$ .

14 Combining the above relations with equation (3.10) we obtain

$$\varepsilon u_{0\tau} \int_{\Omega_g} dz = \left[ \int_{\Omega_g} dz + \int_{\Omega_g} \nabla_z w dz \right] \nabla_y^2 u_0 - \frac{1}{\gamma_u} R(u_0) |\Gamma_c| + f_0 \int_{\Omega_g} dz, \quad (3.11)$$

15 or

$$\varepsilon u_{0\tau} = \left[ 1 + \frac{1}{|\Omega_g|} \int_{\Omega_g} \nabla_z \cdot w dz \right] \nabla_y^2 u_0 - \frac{1}{\gamma_u} \frac{|\Gamma_c|}{|\Omega_g|} R(u_0) + f_0, \quad (3.12)$$

1 for  $|\Omega_g| = \int_{\Omega_g} dz$ .

2 On summarizing the final set of equations that are derived by this process, modelling  
3 corrosion in a macroscopic scale, is

$$\begin{aligned} \varepsilon \frac{\partial u_0}{\partial \tau}(y, \tau) &= D(y, \tau) \nabla_y^2 u_0(y, \tau) - \frac{1}{\gamma_u} \frac{L(y, \tau)}{A(y, \tau)} R(u_0) + f_0 \quad \text{in } \Omega_g, \\ \frac{\partial \mathcal{S}_0}{\partial \tau} \frac{1}{|\nabla_z \mathcal{S}_0|} &= R(u_0) \quad \text{on } \Gamma_c, \\ \frac{\partial \mathcal{Z}_0}{\partial \tau} \frac{1}{|\nabla_z \mathcal{Z}_0|} &= \frac{\partial}{\partial \tau} \left( \sqrt{1 + \frac{1}{4} \gamma_a \int_0^1 (S_0(y, z_1, 0) - S_0(y, z_1, \tau)) dz_1} \right) \quad \text{on } \Gamma_e, \end{aligned}$$

4 for  $D(y, \tau) = \left[ 1 + \frac{1}{|\Omega_g|} \int_{\Omega_g} \nabla_z \cdot w dz \right]$ ,  $A(y, \tau) = \frac{1}{\phi_g} |\Omega_g|$ ,  $L(y, \tau) = \frac{1}{\phi_g} |\Gamma_c|$ .

5 The area  $A(y, \tau)$  is determined as the area between the boundaries  $\Gamma_c$  and  $\Gamma_e$ .

6 Moreover by the fact that to first order terms we have  $\mathcal{S} = z_2 - S(y, z_1, \tau) \simeq \mathcal{S}_0$ ,  
7  $\mathcal{Z} = z_2 - Z(y, z_1, \tau) \simeq \mathcal{Z}_0$  we get

$$\begin{aligned} L(y, \tau) &= \int_{\Gamma_c} dz = 4 \int_0^1 \sqrt{1 + \left( \frac{\partial S}{\partial z_1} \right)^2} dz_1, \\ A(y, \tau) &= 4 \left[ \int_0^1 Z(y, z_1, \tau) dz_1 - \int_0^1 S(y, z_1, \tau) dz_1 \right]. \end{aligned}$$

8 The term  $\int_0^1 \sqrt{1 + \left( \frac{\partial S}{\partial z_1} \right)^2} dz_1$  in the above equation gives the length of the inner boundary  
9 in the first quadrant and therefore to get the full length of the boundary  $L(y, \tau)$  we  
10 multiply by four. The same applies for  $A(y, \tau)$ .

### 11 Overall change in porosity

12 An additional aspect we have to account for, is the change of the porosity  $\phi = \phi(y, \tau)$   
13 during the process and due to the transformation of calcite to gypsum. We must have a  
14 variation of the porosity in one cell from  $\phi_c$  initially (porosity of the uncorroded material)  
15 to  $\phi_g$  (gypsum porosity) at the end of the process. Also the maximum expansion of the  
16 cell area will be achieved when all of the calcium carbonate has been transformed into  
17 gypsum. Furthermore the gypsum created is distributed in such a way so that new void  
18 space (new islets of void space) is created, expanding the total cell area. The additional  
19 final area should be  $\gamma_a \times \text{Initial core area} = \gamma_a(4 - A(y, 0))$  and the total cell area  
20 becomes  $4 + \gamma_a(4 - A(y, 0))$ , for  $\Omega(0) = 4$  and  $4 - A(y, 0)$  the initial calcite core area.

21 The total area of the cell at time  $\tau$ , in terms of  $A(y, \tau)$ , is

$$\begin{aligned} |\Omega|(\tau) &= |\Omega|(0) + \gamma_a (|\Omega_c|(0) - |\Omega_c|(\tau)) = |\Omega|(0) + \gamma_a ((|\Omega|(0) - A(y, 0)) - (|\Omega|(\tau) - A(y, \tau))) \\ &= -\gamma_a |\Omega|(\tau) + (1 + \gamma_a) |\Omega|(0) + \gamma_a (A(y, \tau) - A(y, 0)) \\ &= |\Omega|(0) + (\gamma_a / (1 + \gamma_a)) (A(y, \tau) - A(y, 0)). \end{aligned}$$

22 Therefore we have

$$\begin{aligned} \phi(y, \tau) &= \frac{\text{Initial Void} + \text{Additional void created at time } \tau}{\text{Initial cell volume} + \text{Additional area due to expansion at time } \tau} \\ &= \frac{4\phi_c + \gamma_v (A(y, \tau) - A(y, 0))}{4 + (\gamma_a / (1 + \gamma_a)) (A(y, \tau) - A(y, 0))}, \end{aligned}$$

1 for  $\phi_c = A(y, 0)/4$ ,  $\gamma_v$  a factor to be determined appropriately and for the additional void  
 2 created written in terms of  $(A(y, \tau) - A(y, 0))$ . More specifically we have at the end of the  
 3 process  $\phi_g = \frac{4\phi_c + \gamma_v(4(1 + \gamma_a(1 - \phi_c)) - A(y, 0))}{4 + (\gamma_a/(1 + \gamma_a))(4(1 + \gamma_a(1 - \phi_c)) - A(y, 0))}$ , which gives  $\gamma_v = \frac{\gamma_a}{1 + \gamma_a}\phi_g + \frac{1}{1 + \gamma_a}\frac{\phi_g - \phi_c}{1 - \phi_c}$ .

4 **Boundary conditions**

5 In the following and in order to complete the model equations we need to impose ap-  
 6 propriate boundary conditions. Also we have to take into account the fact that during  
 7 the process, in the macroscale, the porosity changes at each point  $(y, \tau)$ . The derived  
 8 equations account for the actual concentration of  $u$  while the effective concentrations of  
 9 it,  $\bar{u}$ , is given by  $\bar{u} = \phi u$ . The total domain of the material under study is  $\Omega_M$  and we  
 10 may take the boundary of  $\Omega_M$  or part of it, exposed to the ambient concentration of the  
 11 pollutant. In this case we can impose standard Diriclet conditions at the boundary  $\partial\Omega_M$   
 12 of the form  $\bar{u} = \phi u = c(t)$ . Where  $c(t)$  the outer concentration of the pollutant possible  
 13 varying with time during the period of the study. For simplicity we can use an average  
 14 value in place of  $c(t)$  and get  $\bar{u} = \phi u = 1$  after an appropriate scaling of  $u$ .

15 Furthermore in the very common case that we have planar propagation of the corrosion  
 16 the domain  $\Omega_M$  can be taken as a one dimensional and have  $\Omega_M = [0, 1]$ , at  $\tau = 0$ , after  
 17 appropriate scaling.

18 In addition we have expansion of the domain due to its change in the porosity and in  
 19 such a case we have to take  $\Omega_M(\tau) = [-\alpha(\tau), 1]$ , for  $\alpha(\tau)$  expressing the shift of the macro-  
 20 scopic boundary to the left due to swelling. Then we should have  $\phi(-\alpha(\tau), \tau) u(-\alpha(\tau), \tau) =$   
 21 1. At the other end  $y = 1$  we can impose Neumann conditions  $\bar{u}_y = (\phi u)_y = 0$  due to an  
 22 assumption of symmetry (having an one dimensional bar corroded from both ends) or  
 23 due the fact that we have some kind of insulation at this end i.e. a material that cannot  
 24 be corroded for  $y \geq 1$ .

25 **Expansion of the macroscopic boundary**

26 The increase of the porosity of each cell causes the expansion of the volume of that cell  
 27 and therefore at each point  $(y, \tau)$  the change in porosity  $d\phi(y, \tau)$  will cause a correspond-  
 28 ing increase in swelling and specifically in the position of the outer boundary  $\alpha(\tau)$ . By  
 29 summing up these contributions we can obtain an estimation of  $\alpha(\tau)$ . Consequently fol-  
 30 lowing this point of view,  $\alpha(\tau)$  is expected to be proportional to the overall change of  
 31 the porosity of the material, namely we have

$$\alpha(\tau) = \frac{\gamma_a}{1/(1 - \phi_c) + \gamma_a} \int_{-\alpha(\tau)}^1 \frac{\phi(y, \tau) - \phi_c}{\phi_g - \phi_c} dy.$$

32 According to this relation, for  $\phi(y, 0) = \phi_c$  we have  $\alpha(0) = 0$  and when the transformation  
 33 to gypsum is complete, after some time  $\tau_c$ , we expect swelling of size  $\gamma_a(1 - \phi_c)$ . Indeed for  
 34  $\phi(y, \tau) = \phi_g$ , for every  $y \in \Omega_M$  and for time  $\tau \geq \tau_c$  we have  $\frac{\gamma_a}{1/(1 - \phi_c) + \gamma_a}(1 + \alpha(\tau)) = \alpha(\tau)$   
 35 or that  $\alpha(\tau) = \gamma_a(1 - \phi_c)$ .

36 Summarizing, the equations derived, for the case that we consider one dimension in the  
 37 macroscale, and by dropping the subscripts in the notation for  $u$ ,  $\mathcal{S}$  and  $\mathcal{Z}$  since  $u \simeq u_0$ ,  
 38  $\mathcal{S} \simeq \mathcal{S}_0$ ,  $\mathcal{Z} \simeq \mathcal{Z}_0$  we have that the upscaled (limit) model takes the following form:

$$\epsilon u_\tau - D(y, \tau)u_{yy} - f_0(y, \tau) = -\frac{1}{\gamma_u}R(u)\frac{L(y, \tau)}{A(y, \tau)}, \quad -\alpha(\tau) < y < 1, \quad \tau \geq 0, \quad (3.13 a)$$

$$u(-\alpha, \tau) = \frac{1}{\phi(-\alpha, \tau)}, \quad u_y(1, \tau) + \frac{\phi_y(1, \tau)}{\phi(1, \tau)} u(1, \tau) = 0, \quad (3.13 b)$$

$$u(y, 0) = u_a(y), \quad (3.13 c)$$

$$-\frac{\partial S}{\partial \tau} \frac{1}{\sqrt{1 + \left(\frac{\partial S}{\partial z_1}\right)^2}} = R(u), \quad 0 < z_1 < 1, \quad \tau \geq 0, \quad (3.13 d)$$

$$S(y, z_1, 0) = S_a(z_1), \quad \frac{\partial S}{\partial z_1}(y, 0, \tau) = 0, \quad (3.13 e)$$

$$\frac{\partial Z}{\partial \tau} \frac{1}{\sqrt{1 + \left(\frac{\partial Z}{\partial z_1}\right)^2}} = \frac{\partial}{\partial \tau} \sqrt{1 + \frac{1}{4} \gamma_a \int_0^1 (S(y, z_1, 0) - S(y, z_1, \tau)) dz_1},$$

$$1 < z_1 < 1 + \gamma_a, \quad \tau \geq 0, \quad (3.13 f)$$

$$Z(y, z_1, 0) = Z_a(z_1), \quad \frac{\partial Z}{\partial z_1}(y, 0, \tau) = 0, \quad (3.13 g)$$

$$L(y, \tau) = 4 \int_{S(y, z_1, \tau)} dz_{\Gamma_s}, \quad A(y, \tau) = 4 \left[ \int_0^1 Z(y, z_1, \tau) dz_1 - \int_0^1 S(y, z_1, \tau) dz_1 \right], \quad (3.13 h)$$

$$\phi(y, \tau) = \frac{4\phi_c + \gamma_v (A(y, \tau) - A(y, 0))}{4 + (\gamma_a/(1 + \gamma_a)) (A(y, \tau) - A(y, 0))}, \quad (3.13 i)$$

$$\alpha(\tau) = \frac{\gamma_a}{1/(1 - \phi_c) + \gamma_a} \int_{-\alpha(\tau)}^1 \frac{\phi(y, \tau) - \phi_c}{\phi_g - \phi_c} dy. \quad (3.13 j)$$

$$D(y, \tau) = \left[ 1 + \frac{1}{\phi_g A(y, \tau)} \int_{\Omega_g} \nabla_z w(z) dz \right] \quad (3.13 k)$$

$$\nabla_z^2 w_i = 0, \quad \text{in } \Omega_g(y, \tau), \quad w = (w_1, w_2), \quad i = 1, 2, \quad (3.13 l)$$

$$n \cdot \nabla_z w_i = 0, \quad \text{on } \Gamma_e, \quad n \cdot \nabla_z w_i = -n_i, \quad \text{on } \Gamma_c(y, \tau). \quad (3.13 m)$$

Here  $u_a$  is the initial condition for  $u$  and a natural choice to make is to take  $u_a = 0$ . Also  $S_a$  is the initial position of the moving boundary  $\Gamma_c$ , applied to all the cells inside the material, assumed to be independent of  $y$  while for  $\tau > 0$  its position is given by the points  $(z_1, z_2)$  for which we have  $z_2 = S(y, z_1, \tau)$ . Similarly  $Z_a$  is the initial position of  $\Gamma_e$ . The range of  $z_1$  in (3.13 c), (3.13 f) is determined by the fact that  $S$  is shrinking and  $Z$  expanding.

#### 4 Transformation to a fixed domain and variations of the model.

##### Change of time variable in the Eikonal equation

In order to simplify the analysis as well as the numerical treatment of the problem we proceed with a change in time variable in the equations for the moving boundaries (3.13 d), (3.13 f) ([23],[24]).

More precisely in (3.13 c) we set  $\frac{\partial S}{\partial \tau} = \frac{\partial S}{\partial \sigma} \frac{\partial \sigma}{\partial \tau}$ , for  $\sigma$  a new time variable. Thus we obtain

$$-\frac{\partial S}{\partial \sigma} \frac{\partial \sigma}{\partial \tau} = R(u) \sqrt{1 + \left(\frac{\partial S}{\partial z_1}\right)^2}, \quad S(y, z_1, 0) = S_a(z_1), \quad \frac{\partial S}{\partial z_1}(y, 0, \tau) = 0.$$

1 Then we set  $\frac{\partial \sigma}{\partial \tau} = R[u(y, \tau)] = R(y, \tau)$  or

$$\sigma = \sigma(y, \tau) = \int_0^\tau R(y, \tau') d\tau'. \quad (4.1)$$

2 and we obtain a form of the Eikonal equation ( $(\frac{\partial S}{\partial \sigma})^2 - (\frac{\partial S}{\partial z_1})^2 = 1$ ) for  $S = S(z_1, \sigma)$ ,

$$-\frac{\partial S}{\partial \sigma} = \sqrt{1 + \left(\frac{\partial S}{\partial z_1}\right)^2}, \quad 0 < z_1 < 1, \quad \sigma \geq 0, \quad (4.2 a)$$

$$S(z_1, 0) = S_a(z_1), \quad S_{z_1}(0, \sigma) = 0. \quad (4.2 b)$$

4 Similarly for the boundary  $\Gamma_e$ , we obtain for  $Z = Z(z_1, \sigma)$

$$\frac{\partial Z}{\partial \sigma} = \sqrt{1 + \left(\frac{\partial Z}{\partial z_1}\right)^2} \frac{\partial}{\partial \sigma} G(\sigma), \quad 0 < z_1, \quad \sigma \geq 0, \quad (4.3 a)$$

$$\text{for } G(\sigma) = \sqrt{1 + \frac{1}{4}\gamma_a \int_0^1 (S(z_1, 0) - S(z_1, \sigma)) dz_1},$$

$$Z(z_1, 0) = Z_a(z_1), \quad Z_{z_1}(0, \sigma) = 0. \quad (4.3 b)$$

7 **Sandpile Solution for  $\Gamma_e$**

8 Given the assumption that the cells inside the material have the specified form of a  
 9 square, the Eikonal equation for  $\Gamma_e$  attains analytical solutions (sandpile solutions [15],  
 10 [23]). For a square cell, say of side 2, we have  $Z_a(z_1) = 1$ , for  $0 < z_1 < 1$ . Assuming  
 11 that this has the form  $Z = 1 + h(\sigma)$  we obtain that  $\frac{dh}{d\sigma} = \frac{\partial}{\partial \sigma} G(\sigma)$  with  $h(0) = 0$  and  
 12  $G(0) = 1$ . Therefore  $h(\sigma) = G(\sigma) - 1$ ,  $Z(z_1, \sigma) = G(\sigma)$ , or

$$Z(y, z_1, \tau) = G\left(\int_0^\tau R(y, \tau') d\tau'\right). \quad (4.4)$$

13 Note also that due to the symmetry of the square element, we need at  $Z = z_1$ , the  
 14 free boundaries to intersect. Thus we have  $Z = G(\sigma)$  for  $0 \leq z_1 \leq G(\sigma)$ . The mov-  
 15 ing boundary stops to expand for  $\sigma = \sigma_f$  the time needed for  $S$  to vanish and have  
 16  $G(\sigma_f) = \left(\sqrt{1 + \frac{1}{4}\gamma_a \int_0^1 (S(z_1, 0)) dz_1}\right)$ . Then the whole of the square element has been  
 17 transformed into gypsum.

18 This form of  $Z$  imply that in the system (3.13) equations (3.13f), (3.13g) can be  
 19 replaced by (4.4) and in addition the second relation in (3.13h) can also be replaced by

$$A(y, \tau) = 4 \left[ G^2 \left( \int_0^\tau R(y, \tau') d\tau' \right) - \int_0^1 S(y, z_1, \tau) dz_1 \right]. \quad (4.5)$$

20 **Sandpile solutions for the inner boundary**

21 Furthermore given a specific initial interface  $S_a$ , we can obtain analytical solutions of  
 22 equation (4.2) ([23]). In such a case in the end we obtain a non-local in time form of  
 23 equation (3.13 a). For the cases of our interest we present them briefly.

1 **Square Segment.** Assuming that the calcite segment is a square of side  $2L_0$  cantered  
 2 in the cell of initial side 2, such that  $\frac{4-(2L_0)^2}{4} = \phi_c$  or  $L_0 = \sqrt{1-\phi_c}$ , we set  $S_a(z_1) =$   
 3  $S(z_1, 0) = L_0$  for  $0 < z_1 < 1$ . Then, as for the outer boundary  $\Gamma_e$ , the solution of equation  
 4 (4.2) is  $S(z_1, \sigma) = L_0 - \sigma$  for  $0 \leq z_1 \leq L_0 - \sigma$ , or  $S(y, z_1, \tau) = L_0 - \int_0^\tau R(y, \tau') d\tau'$ .

5 Thus for  $L$  and  $A$ , the first of equation(3.13 h), and (4.5) become

$$L(y, \tau) = 8 \left[ L_0 - \int_0^\tau R(y, \tau') d\tau' \right],$$

$$A(y, \tau) = 4 \left[ G^2 \left( \int_0^\tau R(y, \tau') d\tau' \right) - \left( L_0 - \int_0^\tau R(y, \tau') d\tau' \right)^2 \right].$$

6 Substitution of these expressions in (4.6) and applying the transformation from  $y$  to  $r$ ,  
 7 results in a nonlocal in time problem.

8 **Cyclical Segment.** The same can be done for the case that the initial calcite segment  
 9 has the form of a cycle. In such a case  $S_a = S(z_1, 0) = \sqrt{R_0^2 - z_1^2}$ , for  $0 < z_1 < 1$ . Then  
 10 the solution of (4.2) is

$$S(y, z_1, \tau) = \left[ \left( R_0 - \int_0^\tau R(y, \tau') d\tau' \right)^2 - z_1^2 \right]^{\frac{1}{2}},$$

11 for  $0 < z_1 < R_0 - \sigma = R_0 - \int_0^\tau R(y, \tau') d\tau'$ . Therefore we have

$$L(y, \tau) = 2\pi \left[ R_0 - \int_0^\tau R(y, \tau') d\tau' \right]$$

$$A(y, \tau) = 4 \left[ G^2 \left( \int_0^\tau R(y, \tau') d\tau' \right) - \frac{\pi}{4} \left( R_0 - \int_0^\tau R(y, \tau') d\tau' \right)^2 \right].$$

## 12 Transformation to a fixed domain

13 Another aspect that we have to adress in system (3.13) is that in the field equation  
 14 (3.13 a) the domain,  $\Omega_M = [-\alpha(\tau), 1]$  is varying with time. One way to treat this is to  
 15 transform the varying domain to a fixed one. This will allow us also to tackle the problem  
 16 numerically. For this purpose we use the new spatial variable ,  $r$ , by setting

$$r = \frac{y + \alpha(\tau)}{1 + \alpha(\tau)},$$

17 so that  $r = 0$  for  $y = -\alpha(\tau)$  and  $r = 1$  for  $y = 1$ . In addition we have  $\frac{\partial}{\partial y} = \frac{1}{1+\alpha(\tau)} \frac{\partial}{\partial r}$ ,  
 18  $\frac{\partial^2}{\partial y^2} = \frac{1}{(1+\alpha(\tau))^2} \frac{\partial^2}{\partial r^2}$ ,  $u_\tau(y, \tau) = u_\tau(r, \tau) + \dot{\alpha}(\tau) \frac{1-r}{1+\alpha(\tau)} u_r(r, \tau)$  and equation (3.13 a) takes  
 19 the form

$$\epsilon u_\tau + \dot{\alpha}(\tau) \frac{1-r}{1+\alpha(\tau)} u_r - \frac{D(r, \tau)}{(1+\alpha(\tau))^2} u_{rr} - f_0(r, \tau) = -\frac{1}{\gamma_u} R(u) \frac{L(r, \tau)}{A(r, \tau)}, \quad (4.6)$$

20 for  $0 < r < 1$ ,  $\tau \geq 0$ .

21 Moreover with this spatial transform we get an easier to handle, form of equation  
 22 (3.13 j), that is

$$\alpha(\tau) = \frac{\gamma_a}{1/(1-\phi_c) + \gamma_a} \int_0^1 \frac{\phi(r, \tau) - \phi_c}{\phi_g - \phi_c} (1 + \alpha(\tau)) dr$$



1 or

$$\alpha(\tau) = \frac{\Phi(\tau)}{\frac{1/(1-\phi_c)+\gamma_a}{\gamma_a} - \Phi(\tau)}, \quad \text{for} \quad \Phi(\tau) = \frac{\int_0^1 \phi(r, \tau) dr - \phi_c}{\phi_g - \phi_c}. \quad (4.7)$$

2 Finally the first of the boundary conditions, (3.13 b) holds for  $r = 0$  while the second  
3 of them remains invariant, namely

$$u(0, \tau) = \frac{1}{\phi(0, \tau)}, \quad u_r(1, \tau) + \frac{\phi_r(1, \tau)}{\phi(1, \tau)} u(1, \tau) = 0, \quad (4.8)$$

4 These equations (4.6), (4.8), (in place of (3.13 a), (3.13 b)) and (3.13 c) for  $u$ , with  
5 the improved form of the equations for the moving boundaries, (4.1), (4.2), (in place of  
6 (3.13 d), (3.13 e)) and (4.4) (in place of (3.13 f), (3.13 g)), the first of (3.13 h) and (4.5) for  
7 the gypsum area, equation (3.13 i) for the porosity  $\phi$ , equation (4.7) for the macroscopic  
8 moving boundary (in place of (3.13 j)) together with (3.13 k), (3.13 l) and (3.13 m), form  
9 the transformed to a fixed domain, model.

## 10 5 Numerical Solution

11 We treat numerically the problem by following similar methodology as in [23], [24]. We  
12 apply a process in three stages.

13 Initially, we need to solve the Eikonal equation (4.2) for the cases that we cannot  
14 obtain an analytical solution. This can be done by using a level set method for a time  
15 range  $0 \leq \sigma \leq \sigma_f$ .

16 At a second stage having obtain the solution for the inner boundary we need to solve  
17 the auxiliary cell problems, i.e. equations (3.13 l), (3.13 m), for a sequence of domains  
18  $\Omega_g(y, \sigma_i)$ , where  $\sigma_i$  correspond to the points of a partition of  $[0, \sigma_f]$ . This is done with a  
19 finite element method.

20 Finally we use these solutions,  $S$  and  $w$ , to evaluate the source terms in the macroscopic  
21 equation for  $u$  and to solve the resulting problem via an implicit in time finite element  
22 scheme.

### 23 Level set method for the Eikonal equation

24 We take a partition of  $[-1, 1] \times [-1, 1]$  of  $(M_\sigma + 1)^2$  points  $z_{1,2,j} = j\delta z_{1,2}$ , with  $\delta z_1 = \delta z_2$ ,  
25 being the spatial steps and for  $j = 0, 1, 2, \dots, M_\sigma$ . Let  $T_\sigma$  being the final time of the  
26 simulation. Similarly in the interval  $[0, T_\sigma]$ , we take a partition with  $N_\sigma$  time steps of  
27 size  $\delta\sigma$  for  $N_\sigma = \lceil \frac{T_\sigma}{\delta\sigma} \rceil$  and  $\sigma_\ell = \ell\delta\sigma$ ,  $\ell = 1, 2, \dots, N_\sigma$ .

28 We denote with  $S_{i,j}^\ell$  the approximation of  $S(z_{1i}, z_{2j}, \sigma_\ell)$ ,  $i, j = 0, 1, 2, \dots, M_\sigma$ ,  $\ell =$   
29  $1 \dots N_\sigma$ . According to a level set method (see [19],[25]), and recalling that  $\mathcal{S} = z_2 -$   
30  $S(y, z_1, \tau)$ , with  $\frac{\partial \mathcal{S}}{\partial \sigma} = |\nabla_z \mathcal{S}|$  we have

$$\begin{aligned} D_{z_1}^+ \mathcal{S}_{i,j}^\ell &= (\mathcal{S}_{i+1,j}^\ell - \mathcal{S}_{i,j}^\ell) / \delta z_1, & D_{z_1}^- \mathcal{S}_{i,j}^\ell &= (\mathcal{S}_{i,j}^\ell - \mathcal{S}_{i-1,j}^\ell) / \delta z_1, \\ D_{z_2}^+ \mathcal{S}_{i,j}^\ell &= (\mathcal{S}_{i,j+1}^\ell - \mathcal{S}_{i,j}^\ell) / \delta z_2, & D_{z_2}^- \mathcal{S}_{i,j}^\ell &= (\mathcal{S}_{i,j}^\ell - \mathcal{S}_{i,j-1}^\ell) / \delta z_2, \\ H &= \sqrt{\min(0, D_{z_1}^- \mathcal{S}_{i,j}^\ell)^2 + \max(0, D_{z_1}^+ \mathcal{S}_{i,j}^\ell)^2 + \min(0, D_{z_2}^- \mathcal{S}_{i,j}^\ell)^2 + \max(0, D_{z_2}^+ \mathcal{S}_{i,j}^\ell)^2}, \\ \mathcal{S}_j^{\ell+1} &= \mathcal{S}_j^\ell - \delta\sigma H \quad i, j = 1 \dots, M_\sigma - 1, \quad \ell = 1 \dots N_\sigma. \end{aligned} \quad (5.1)$$

1 For the stability of the above scheme the condition  $(\delta\sigma/\delta z_1 + \delta\sigma/\delta z_2) \leq 1/2$  should be  
 2 satisfied. In Figure 3 we plot the numerical solution of the Eikonal equation in the case  
 3 that we have as an initial curve a Lamé curve of the form  $z_1^n + z_2^n = C$  ([16]). The curve  
 shrinks towards the center of the square.

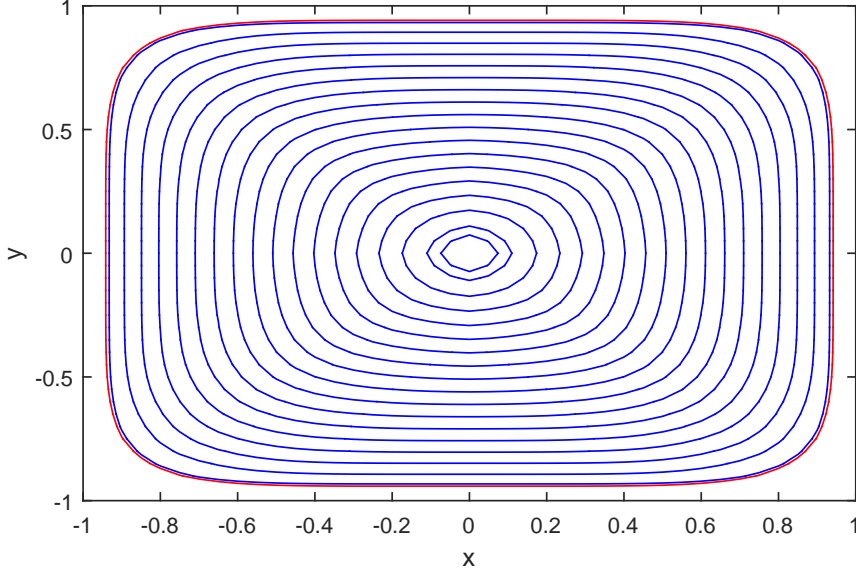


FIGURE 3. Numerical solution for the Eikonal equation. The initial curve (red line) is  $z_1^n + z_2^n = C$  for  $n = 6$  and  $C = 0.7$ . The solution is plotted for various times. As time increases the curve shrinks towards the center of the cell. Here  $\delta z_{1,2} = 0.05$ ,  $\delta\sigma = 0.0075$ .

4  
 5 This solution must be expressed in terms of the time variable  $\tau$ . In order to do so we  
 6 take a grid for the macroscopic domain  $[0, T] \times [0, 1]$ . We have for  $0 \leq \tau \leq T$ ,  $\tau_n = n\delta\tau$ ,  
 7  $\delta\tau = [\frac{T}{N}]$  and for  $N$  the time steps. Also for  $0 \leq r \leq 1$  we take  $M + 1$  points  $r_j = j\delta r$ ,  
 8  $j = 0, 1, \dots, M$  for  $\delta r$  the spatial step.

9 Given the approximation of  $\mathcal{S}(z_1, z_2, \sigma) = z_2 - S(z_1, \sigma)$  at the point  $(z_{1j}, \sigma_\ell)$ ,  $S_j^\ell$ , in  
 10 terms of  $\sigma$  (restricted in the quarter domain  $[0, 1] \times [0, 1]$  due to symmetry), with  $S^\ell :=$   
 11  $(S_1^\ell, S_2^\ell, \dots, S_{M_\sigma}^\ell)$ , we are able to calculate the quantities  $L$  and  $A$  in the source term  
 12 in the equation for  $u$  at each time step. We determine (interpolate) for each  $(r_j, \tau_i)$  the  
 13 corresponding  $\sigma_\ell$  so that  $A(r_j, \tau_i) = I_A(\sigma_\ell) := \int_0^1 S(z_1, \sigma_\ell) dz_1$  and  $L(r_j, \tau_i) = I_L(\sigma_\ell) :=$   
 14  $\int_{S^\ell} S(z_1, \sigma_\ell) dz_1$ . The index  $\ell$  of  $\sigma_\ell$  that corresponds to the point  $(r_j, \tau_i)$  is the one that  
 15 minimizes the quantity  $(\sigma_\ell - I_{\tau_i}^j)$ , for  $I_{\tau_i}^j := \int_0^{\tau_i} R(r_j, \tau') d\tau'$ .

#### 16 Finite element method for the cell problems

17 The next stage is to solve numerically the cell problems for  $w$ , (3.13 k) and (3.13 l). We  
 18 have obtained the solution of the Eikonal equation. Namely we know the position of the  
 19 inner boundary  $S$  together of course with the position of the outer boundary  $Z$ . This  
 20 allow us to identify at each time step  $\sigma_\ell$ , in a partition of the interval  $[0, T_\sigma]$ , the domain  
 21  $\Omega_g = \Omega_g(\sigma)$ . Then for this domain we use a finite element scheme to solve these cell

1 problems. The finite element numerics package in MATLAB "Distmesh" ([26]) is used  
 2 to triangulate  $\Omega_g(\sigma)$ . Then a solver that has been implemented for this specific problem  
 3 (equations (3.13 k), (3.13 l)) is applied. An example of such a numerical solution for this  
 problem is presented in Figure 4.

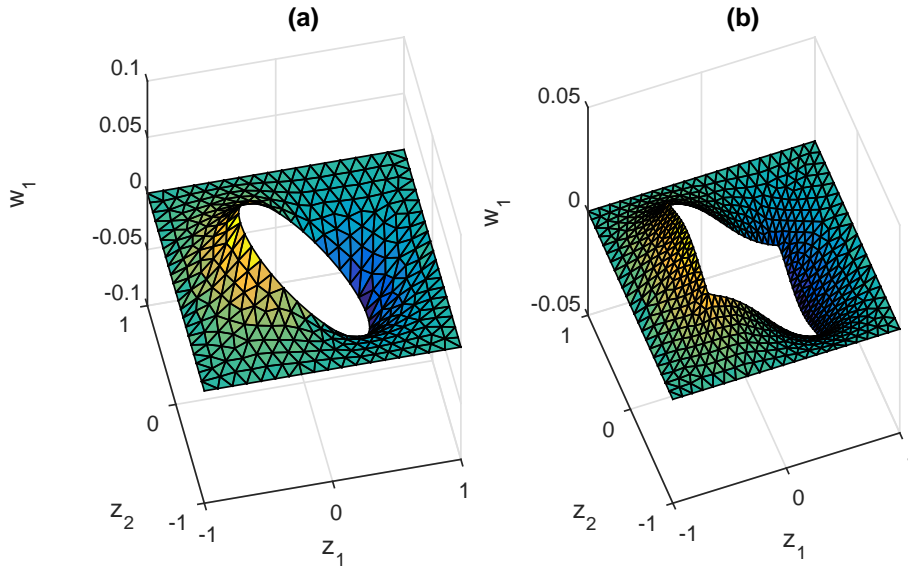


FIGURE 4. Numerical solution via a finite element method for a cell problem. In (a) the problem (3.13 k) and (3.13 l), for  $w_1$  is solved in the case that the inner boundary is a circle of radius  $R = 0.5$ . In (b) the same problem is solved in the case that the inner interface is a square of side  $2L_0 = 0.5$ .

4  
 5 As a next step we can evaluate the variable diffusion coefficient given by equation  
 6 (3.13 k). In the graphs of Figure 5 we can see the variation of  $D(y, \tau)$  against the gypsum-  
 7 void area  $|\Omega_g|$ . In the case that the initial calcite core (inner boundary) is taken to be a  
 8 circle or a square, the analytical sandpile solution is used. For the case that the initial  
 9 calcite core is taken with a form that we cannot have analytical solution of the Eikonal  
 10 equation, for example a Lamé curve with equation  $z_1^n + z_2^n = C$  as in Figure 3, it uses  
 11 the numerical solution obtained with a level set method. In this way the positions of the  
 12 inner boundary is determined and consequently  $|\Omega_g|$ . In the latter case and for a Lamé  
 13 curve the initial area is given by  $\sqrt{\frac{\Gamma(1+2/n)}{4\Gamma(1+1/n)}}$ . The expansion of the outer cell boundary  
 14 given by the relevant sandpile solution is also considered in all of the above cases.

#### 15 Finite element scheme for the field equations

16 In the third stage we use a finite element scheme to solve the field equation (4.6) together  
 17 with its boundary and initial conditions. Let  $\psi_j = \psi_j(r)$ ,  $j = 0, \dots, M$  denote the  
 18 standard linear B - splines on the interval  $[0, 1]$ , defined with respect to the partition  
 19 considered. We then set  $u(r, \tau) = \sum_{j=0}^M a_{u_j}(\tau)\psi_j(r)$ ,  $\tau \geq 0$ ,  $0 \leq r \leq 1$ . We apply the  
 20 standard Galerkin method and obtain a system of equations for the  $a$ 's. We also denote

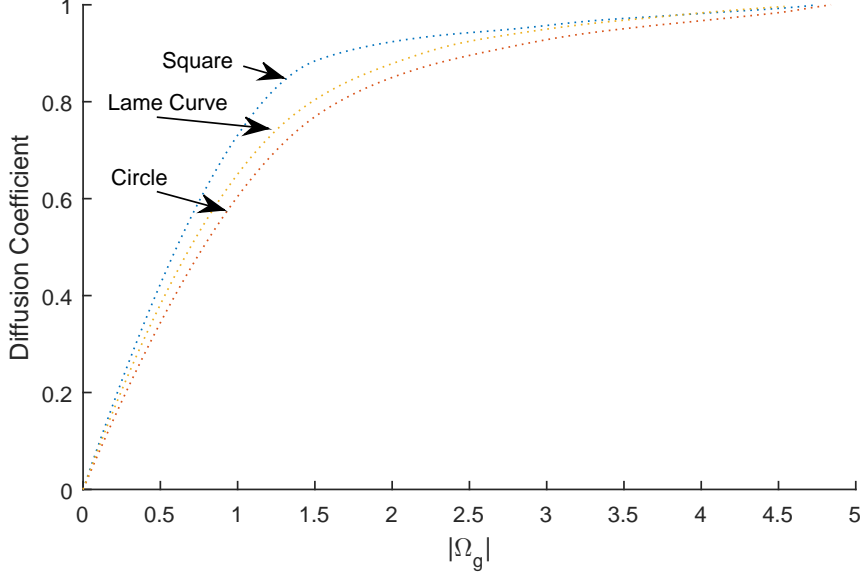


FIGURE 5. Numerical estimation of the diffusion coefficient  $D$  given by equation (3.13k) against  $|\Omega_g|$ . The diffusion coefficient is plotted for the cases that the initial calcite core is a square, a circle and a Lamé curve.

1 by  $F$ , the source term in the equation for  $u$ . Specifically  $F(u) := -1/\gamma_u \times R(u) L/A + f_0$ .

$$\begin{aligned}
 \epsilon \sum_{j=0}^M \dot{a}_{u_j} \int_0^1 \psi_j \psi_i dr &= -\frac{1}{(1+\alpha)^2} \sum_{j=0}^M a_{u_j} \int_0^1 D(r, \tau) \psi_j' \psi_i' dr - \frac{\dot{\alpha}}{1+\alpha} \sum_{j=0}^M a_{u_j} \int_0^1 (1-r) \psi_j' \psi_i dr \\
 &\quad + \int_0^1 F \left( \sum_{j=0}^M a_{u_j} \psi_j \right) \psi_i dr, \tag{5.2}
 \end{aligned}$$

2 where  $i = 1, 2, \dots, M$ . Setting  $a_u = [a_{u_1}, a_{u_2}, \dots, a_{u_M}]^T$  the system of equations for the  
3  $a_u$ 's takes the form

$$B_l \dot{a}(\tau) = -\frac{1}{(1+\alpha(\tau))^2} B_r(\tau) a(\tau) - \frac{\dot{\alpha}(\tau)}{1+\alpha(\tau)} C a(\tau) + b_u(\tau),$$

4 The matrices

5  $B_l := \left( \int_0^1 \psi_j(r) \psi_i(r) dr \right)$ ,  $B_r := \left( \int_0^1 D(r, \tau) \psi_j'(r) \psi_i'(r) dr \right)$  and  $C := \left( \int_0^1 (1-r) \psi_j'(r) \psi_i(r) dr \right)$   
6 have the standard form in this case (e.g. see [22], [23]) and  $b_u$ , is the array coming from  
7 the last term in equation (5.2).

8 For the resulting system of ODE's we apply an implicit scheme and take

$$\left[ B_l + \delta\tau \frac{1}{(1+\alpha(\tau_n))^2} B_r(\tau_n) + \delta\tau \frac{\dot{\alpha}(\tau_n)}{1+\alpha(\tau_n)} C - \delta\tau \bar{b}_u(\tau_n) \right] a_u^{n+1} = B_l a_u^n. \tag{5.3}$$

9 Some extra care is needed for the evaluation of  $\alpha^{n+1} \simeq \alpha(\tau_{n+1})$  and of  $\dot{\alpha}(\tau_{n+1}) \simeq$

$(\alpha^{n+1} - \alpha^n)/\delta\tau$ . We have that  $\alpha(\tau) = \Phi(\tau)/\left(\frac{\gamma_a}{1/(1-\phi_c)+\gamma_a} - \Phi(\tau)\right)$  and that

$$\dot{\alpha}(\tau) = \frac{\frac{\gamma_a}{1/(1-\phi_c)+\gamma_a} \dot{\Phi}(\tau)}{\left(\frac{\gamma_a}{1/(1-\phi_c)+\gamma_a} - \Phi(\tau)\right)^2}, \quad \dot{\Phi}(\tau) = \frac{1}{\phi_g - \phi_c} \frac{d}{d\tau} \int_0^1 \frac{4\phi_c + \gamma_v (A(r, \tau) - A(r, 0))}{4 + \gamma_a/(1 + \gamma_a) (A(r, \tau) - A(r, 0))} dr.$$

Then we use the approximation  $\frac{d}{d\tau} \Phi(\tau_n) \simeq (\Phi(\tau_n) - \Phi(\tau_{n-1}))/\delta\tau$ .

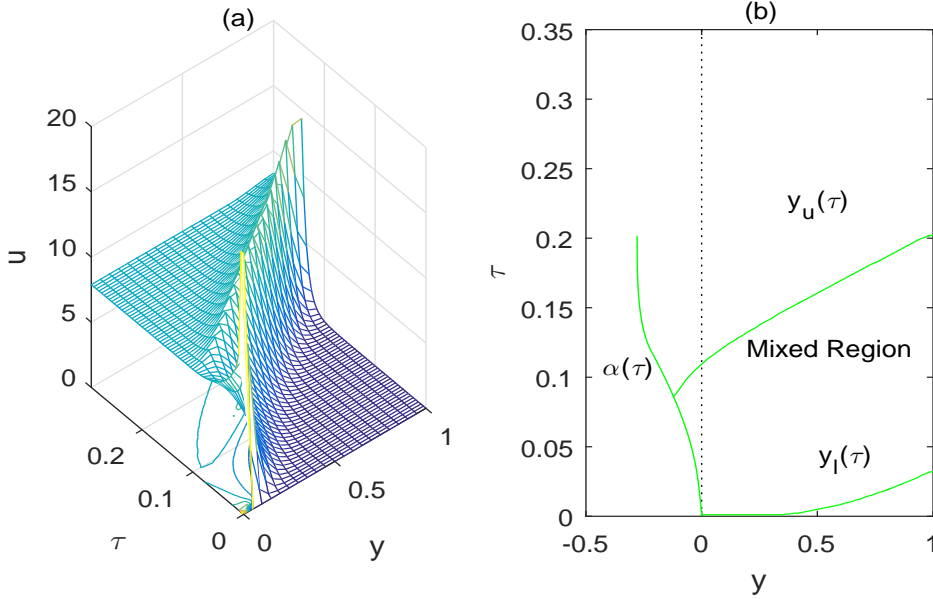


FIGURE 6. Numerical solution of the system (3.13). In (a) the variable  $u$  is plotted against space and time and in (b) the moving boundaries, indicating when the corrosion is complete in the case of having an initial calcite element in the form of a square.

In Figure 6 the system of equations (3.13) is solved numerically for the case that the initial shape of the calcite core is a square. In (a)  $u$  is plotted against space and time. In (b) the moving boundaries,  $y_l(\tau)$  and  $y_u(\tau)$ , given by the conditions:  $\max\{\tau : A(y_l(\tau), \tau) = 4 - (2L_0)^2\}$  and  $\min\{\tau : A(y_u(\tau), \tau) = 4(1 + \gamma_a L_0^2)\}$  respectively, are plotted against time (in the vertical axes) together with  $\alpha(\tau)$ . The values of the parameters used in these simulations are for  $M = 61$ ,  $T = .8$ ,  $\epsilon = 1$ ,  $\gamma_m = 1$ ,  $\rho_c = 2.71\text{gr/cm}^3$ ,  $\rho_g = 2.31\text{gr/cm}^3$ ,  $\rho_m = 0.7352$ ,  $\phi_c = 0.05$ ,  $\phi_g = 0.15$ ,  $\delta\tau = .8 \cdot \delta y^2$ . The area between  $y_l$ ,  $y_u$  and  $\alpha(\tau)$  specifies the region where the corrosion process is taking place and pure calcite and gypsum coexist in a microscopic scale.

### 5.1 Application for the case of a limestone monument corrosion.

In such a case the reaction (2.2) applies. We proceed with the modelling approach described in [24].

We describe briefly the model by focusing in the minor modification needed to add in the equations already presented. According to the reaction (2.2) we have that the

1 the molar concentration of  $\text{SO}_4^{2-}$ ,  $u$  satisfies the diffusion equation in the pores of the  
2 material

$$\epsilon_1 u_\tau = \Delta u. \quad (5.4)$$

3 We also have diffusion of water of dimensionless concentration  $v = v(y, \tau)$  in the same  
4 domain and

$$\epsilon_2 v_\tau = \Delta v. \quad (5.5)$$

5 The motion of the boundary, the inner surface of the pore is given by the standard kinetic  
6 condition expressing the fact that *Speed of the moving boundary*  $\times$  *Calcium carbonate*  
7 *concentration*  $\propto$  *Rate of reaction*. In our case and by taking into account the Law of mass  
8 action we have that the rate of reaction should have the form

$$R(y, \tau) = g(v)uv^2.$$

9 The function  $g$  models the fact that the reaction takes its full speed when the water  
10 concentration is larger than an upper threshold  $v_u$  and it does not occur at all when the  
11 concentration is lower than a lower threshold  $v_l$ . Between  $v_l$  and  $v_u$  we have to account  
12 for the fact that calcium carbonate inside the pores is covered just by water droplets  
13 and not of a water film and thus reaction takes place but not in its full speed. Such a  
14 function should have the form  $g(v) = \frac{\min(\max(v, v_l), v_u) - v_l}{v_u - v_l}$  ([24]). Thus at the boundary  
15  $\Gamma_M$  the kinetic condition for the speed of the moving boundary  $\mathbf{V}$  should be

$$\mathbf{V} = R(y, \tau), \quad y \in \Gamma_M. \quad (5.6)$$

16 Furthermore the flux of  $u$  arriving at the interface is consumed by the chemical reaction  
17 transforming concrete into gypsum. In addition we may have transport of the residual  
18 reactant due to the motion of the boundary and thus the boundary condition at the  
19 interface of the corroded - uncorroded material, given that  $\mathbf{V} = R(y, \tau)$  will be

$$\gamma_1 \frac{\partial u}{\partial n} = \mathbf{V} + \beta_1 \mathbf{V}u, \quad y \in \Gamma_M, \quad (5.7)$$

20 where  $n$  is the outward normal vector at a point of the moving boundary  $\Gamma_M$  and for  
21  $\gamma = \gamma_u \frac{1}{\delta}$ . The same should apply for the water concentration  $v$  and get

$$\gamma_2 \frac{\partial v}{\partial n} = 2\mathbf{V} + \beta_2 \mathbf{V}v, \quad y \in \Gamma_M. \quad (5.8)$$

22 These equations apply in the porous net inside the material in  $\Gamma_M$ . Moreover we  
23 consider exactly the same geometry and setting as the one described in section 2. In the  
24 cell symmetry conditions should be applied for the variable  $u$  and  $v$  in the following form:

$$n \cdot \nabla u|_{\partial\Omega} = 0, \quad n \cdot \nabla v|_{\partial\Omega} = 0 \quad y \in \Gamma_e. \quad (5.9)$$

25 The expansion of the cell boundary is given again by :

$$\mathbf{V}_e = \frac{\partial}{\partial \tau} \left( \sqrt{|\Omega(0)| + \gamma_a A_g(\tau)} \right), \quad y \in \Gamma_e. \quad (5.10)$$

26 As we can see the additions in the basic model of section 3 is that we consider also  
27 diffusion of the water and an extra equation for it, together with the specific form of  
28 the reaction term  $R = R(u, v)$ . Also there is no production of  $u$  inside the material i.e.

1  $f \simeq f_0 = 0$  and transport of the residual reactant gives an extra term in the boundary  
 2 conditions at  $\Gamma_M$ . The homogenization analysis can be carried out in exactly the same  
 3 way and finally we can obtain the full system of equations to be solved. Namely, for  
 4  $\epsilon_i, \beta_i, \gamma_i, i = 1, 2$ , dimensionless constants ([24]), the equation for  $u$  is

$$\epsilon_1 u_\tau - D(y, \tau) u_{yy} = -\frac{1}{\gamma_u} R(u, w) (1 + \beta_1 u) \frac{L(y, \tau)}{A(y, \tau)}, \quad -\alpha(\tau) < y < 1, \quad \tau \geq 0 \quad (5.11 a)$$

$$u(-\alpha, \tau) = \frac{1}{\phi(-\alpha, \tau)}, \quad u_y(1, \tau) + \frac{\phi_y(1, \tau)}{\phi(1, \tau)} u(1, \tau) = 0, \quad (5.11 b)$$

$$u(y, 0) = u_a(y), \quad (5.11 c)$$

7 while the diffusion equation for the water concentration  $v$  has the form,

$$\epsilon_2 v_\tau - D(y, \tau) v_{yy} = -\frac{1}{\gamma_w} R(u, v) (2 + \beta_2 v) \frac{L(y, \tau)}{A(y, \tau)}, \quad -\alpha(\tau) < y < 1, \quad \tau \geq 0, \quad (5.12 a)$$

$$v(-\alpha, \tau) = \frac{1}{\phi(-\alpha, \tau)}, \quad v_y(1, \tau) + \frac{\phi_y(1, \tau)}{\phi(1, \tau)} v(1, \tau) = 0, \quad (5.12 b)$$

$$v(y, 0) = v_a(y), \quad (5.12 c)$$

10 together with the equation for the motion of the inner boundary, (3.13 d), (3.13 e), but  
 11 with  $R = R(u, v)$ , as already defined, instead of  $R = R(u)$ , and the equations for the  
 12 motion of the outer boundary (3.13 f), (3.13 g). In addition  $L$  and  $A$  are determined  
 13 by equation (3.13 h), the porosity  $\phi$  by (3.13 i), the expansion of the macroscopic outer  
 14 boundary by (3.13 j), the variation of the diffusion coefficient by (3.13 k) while the cell  
 15 problems are given by equations (3.13 l) and (3.13 m).

16 The rest of the analysis of section 3 can be easily adjusted to this case. The form of  
 17  $\Gamma_e$  will be given in the same way. Additionally the problem has to be transformed to a  
 18 fixed domain and the left hand side of equations (5.11 a), (5.12 a) takes a form similar to  
 19 the left hand side of equation (4.6).

20 We use values for the parameters taken by [7], [24] and we have  $\epsilon_1 = 1.01 \cdot 10^{-12}$ ,  
 21  $\epsilon_2 = 6.9964 \cdot 10^{-13}$ ,  $\gamma_u = 5.98$ ,  $\gamma_w = 1.2685 \cdot 10^{13}$ ,  $\beta_1 = 5.053 \cdot 10^{-12}$  and  $\beta_2 = 6.1131 \cdot 10^{-6}$ ,  
 22  $\gamma_a = 0.3276$ .

23 Therefore the water diffusion is very fast compared with the reaction progress. Thus  
 24  $v_{yy} \simeq 0$  for  $\epsilon_2, 1/\gamma_w \ll 1$ . For a constant concentration at the boundary  $y = 0$ ,  $v\phi = 1$   
 25 and  $(v\phi)_y = 0$ , at the point  $y = 1$ , and as far as  $D(y, \tau) = O(1)$ ,  $v$  is approximated by

$$v = \frac{1}{\phi(0, \tau)} \left[ 1 - \frac{\phi_y(1, \tau)}{\phi(1, \tau) + \phi_y(1, \tau)} y \right]. \quad (5.13)$$

26 Moreover the equation for  $u$ , given that  $\epsilon_1, \beta_1 \ll 1$ , is approximated by

$$D(y, \tau) u_{yy} = \frac{1}{\gamma_u} g(v) u v^2 \frac{L(y, \tau)}{A(y, \tau)}, \quad -\alpha(\tau) < y < 1, \quad \tau \geq 0. \quad (5.14)$$

27 Therefore the quasi steady approximation is valid for the system. For this case a sim-  
 28 ulation has been done in Figure 7 where the boundaries  $y_u$  and  $y_l$  are plotted against  
 29 time and  $S_a$  is taken to be a) a square, b) a circle, c) a Lamé curve. We can see that  
 30 due to the fact that diffusion is fast a layer of thickness  $y = 1$  ( $x = l = .012$  cm), in-  
 31 stantly becomes partly corroded, i.e.  $y_l$  is placed very close at the  $\tau = 0$  line, while this  
 32 layer is fully corroded at about 0.0025 time units for a circular calcite core or at about

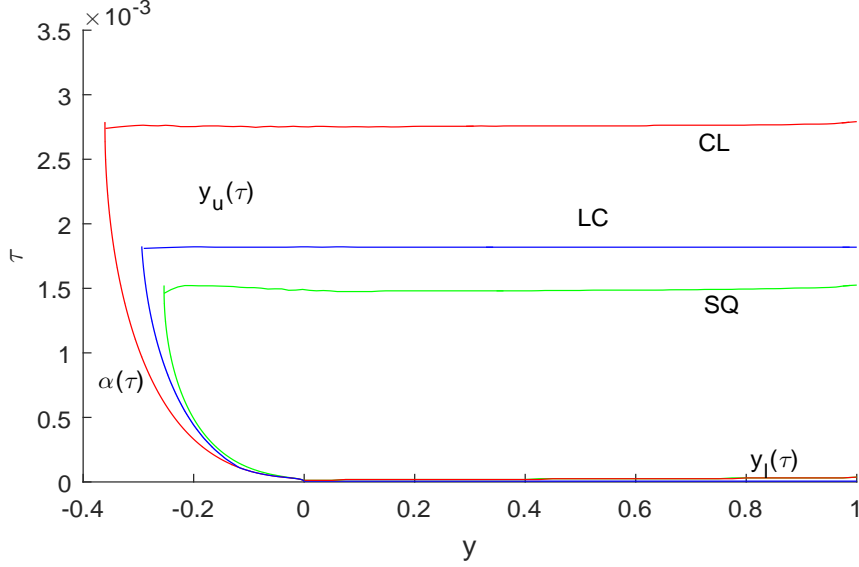


FIGURE 7. A simulation of the corrosion process for the case that we have equations (5.14) and (5.13) in place of (5.11 a) and (5.12 a) together with the rest of the equations of the system (3.13), for small  $\epsilon_2$  and  $1/\gamma_w$ . The simulations are done in the case that we have in the microgeometry a) a square shaped core (SQ, green line) b) a circle shaped calcite core (CL, red line) and c) a Lame curve shaped core (LC, blue line).

1  $t = 0.0025 \times t_0 \simeq 1$  month for the timescale  $t_0$  used. Corrosion is faster in the case  
 2 of a Lame curve - geometry and even faster for square cell geometry The effect of the  
 3 microgeometry in the process is apparent here.

## 4 5.2 Application for the case of sewers pipes corrosion.

5 In the case of sewers pipes corrosion we have that  $H_2S$ , which is produced inside the pipes  
 6 diffuses inside the pores of the pipe wall from its inner surface and through in it. Then  
 7 inside the pores of the pipe wall we have  $H_2S$  in the gaseous phase with dimensionless  
 8 concentration  $v_g$ ,  $H_2S$  in the liquid phase and of dimensionless concentration  $v_l$ , coexist-  
 9 ing. These are exchanged between gaseous and liquid phase. Moreover the liquid  $H_2S$  due  
 10 to bioconversion is transformed to  $SO_4^{2-}$ , of dimensional concentration  $u$ , which in tern  
 11 reacts with the calcite of the inner wall of the pore producing gypsum  $CaSO_4 \cdot 2H_2O$ .  
 12 The latter process, which actually is the cause of the corrosion, is described by the  
 13 reaction (2.1).

14 The equations in dimensionless form expressing the evolution of the concentrations  
 15 inside the pores of the material(see [5], [22], [23]) are

$$\epsilon_1 \frac{\partial v_g}{\partial \tau} = \frac{\partial^2 v_g}{\partial y^2} - \mu_1 (\beta_1 v_g - v_l), \quad (5.15 a)$$

$$\epsilon_2 \frac{\partial v_l}{\partial \tau} = \frac{\partial^2 v_l}{\partial y^2} + \mu_2 (\beta_1 v_g - v_l) - \beta_2 v_l, \quad (5.15 b)$$



$$\epsilon_3 \frac{\partial u}{\partial \tau} = \frac{\partial^2 u}{\partial y^2} + \beta_3 v_l, \quad (5.15 c)$$

1 with  $\epsilon_i, \beta_i, i = 1, 2, 3, \mu_1, \mu_2$  dimensionless constants ([22]). The motion of the moving  
2 boundary inside the pore of the material is given by (3.13 d), (3.13 e), but with

$$R(y, \tau) = u, \quad y \in \Gamma_M. \quad (5.16)$$

3 After applying the averaging process in the same way as before and having in mind that  
4 for  $v_g$  and  $v_l$  Neumann conditions hold for the moving boundary  $\Gamma_c$ , we obtain for the  
5 macroscopic scale

$$\epsilon_1 \frac{\partial v_g}{\partial \tau} = D(y, \tau) \frac{\partial^2 v_g}{\partial y^2} - \mu_1 (\beta_1 v_g - v_l), \quad (5.17 a)$$

$$\epsilon_2 \frac{\partial v_l}{\partial \tau} = D(y, \tau) \frac{\partial^2 v_l}{\partial y^2} + \mu_2 (\beta_1 v_g - v_l) - \beta_2 v_l, \quad (5.17 b)$$

$$\epsilon_3 \frac{\partial u}{\partial \tau} = D(y, \tau) \frac{\partial^2 u}{\partial y^2} + \beta_3 v_l + F(u) \quad (5.17 c)$$

8 for  $F(u) = -\frac{1}{\gamma_u} R(u) \frac{L(y, \tau)}{A(y, \tau)}$  as in equation (3.13 a) while the same equations (3.13 d)-  
9 (3.13 l) apply as before. Note also that here in equation (5.17 c) the term  $\beta_3 v_l$  plays the  
10 role of  $f$  in equation (3.13 a). This set of equations can be completed with appropriate  
11 boundary and initial conditions of the form (3.13 b) and (3.13 c) for all concentrations  
12  $v_g, v_l, u$ .

13 In the case that we evaluate the dimensionless constants with specific values of the  
14 parameters (cf. [5, 22]) we may obtain small values for  $\epsilon$  and large values for  $\mu$ . More  
15 specifically, we have  $\epsilon_1, \epsilon_2, \epsilon_3 \ll 1$  and  $\mu_1, \mu_2 \gg 1, \beta_1 = 1$ , giving  $v_g \sim v_l$  and allowing  
16 us to apply again a quasi steady approximation. In such a case the model equations to  
17 be solved become

$$D(y, \tau) \frac{\partial^2 v_l}{\partial y^2} - \beta_2 v_l = 0, \quad (5.18 a)$$

$$D(y, \tau) \frac{\partial^2 u}{\partial y^2} + \beta_3 v_l + F(u) = 0. \quad (5.18 b)$$

19 A simulation is presented in Figure 8. We notice some small variations between the  
20 boundaries with respect to the considered microstructure geometry (square, circle or  
21 Lamé curve shaped calcite core). The corrosion is faster in the case of the square-cell  
22 geometry. The effect of diffusion is fast, the material becomes immediately everywhere  
23 partly corroded and fully corroded simultaneously at a later time. The material is fully  
24 transformed, e.g. for the case of circle, at about 0.1328 time units which in dimensional  
25 terms gives that a layer of 13 cm is fully corroded after 22.67 years.

## 26 6 Discussion

27 The major issue in the present paper is to expand an existing model, describing calcium  
28 carbonate corrosion and addressing also the formation of a mixed (mushy) region during  
29 this process. The modelling expansions include the phenomenon of volume expansion  
30 coming from the difference in the density of calcite and gypsum as well as the variation

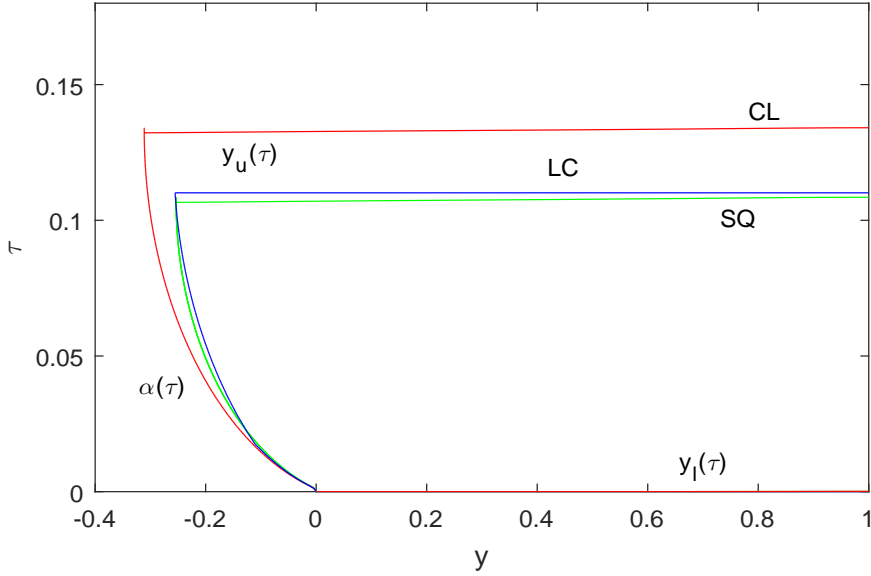


FIGURE 8. A simulation of the corrosion process for the case that we have equations (5.18 a) and (5.18 b) in place of (5.17 b) and (5.17 c) together with the rest of the equations in the system (5.17), for small  $\epsilon_2, \epsilon_3$  and a square (green line), circular (red line) or Lame curve (blue line) shaped calcite core in the microgeometry. In general there is visible difference in the final result regarding the microstructure consideration. We observe faster corrosion in the case of square cell and slower in the case of a cyclic cell. For a cell shaped as a lame curve the behaviour is intermediate.

1 of the diffusion behaviour resulting from the shape evolution of the calcite part inside a  
 2 pore. Homogenization method is applied to derive a set of macroscopic equations which  
 3 can be solved numerically.

4 In some cases the complete set of the resulting equations can be simplified so that to  
 5 diminish the numerical complications. For the same reason in the microscale only two  
 6 dimensional geometry is considered. Some simulations for various cases are presented.

7 An important aspect to be addressed in a future work should be the study of existence,  
 8 uniqueness and asymptotic of the properties of the solution of the macroscopic model  
 9 derived in this work.

10 Of course further extensions of this work, regarding the modelling approach and  
 11 the derivation of macroscopic equations, should include three dimensional microscale  
 12 geometry. Another aspect avoided at the present and of possible future research, is to  
 13 include in the model the stress forces between the cells and due to volume expansion. Also  
 14 additional simulations for different macroscopic geometries could be another interesting  
 15 aspect. Moreover this model can be adjusted to other similar phenomena where we have  
 16 corrosion in a porous media.

#### 17 Acknowledgements

18 The author wants to express his gratitude to the anonymous reviewers and especially

1 reviewer # 1 for his valuable and important remarks regarding various aspects of this  
2 work.

### References

- 3
- 4 [1] G. Ali, V. Furuholt, R. Natalini and I. Torcicollo, (2007) *A mathematical model of sulphite*  
5 *chemical aggression of limestones with high permeability. Part I. Modeling and qualitative*  
6 *analysis, Transport in Porous Media*, **69**, 109–122.
- 7 [2] G. Ali, V. Furuholt, R. Natalini and I. Torcicollo, (2007) *A mathematical model of sulphite*  
8 *chemical aggression of limestones with high permeability. Part II: Numerical approxima-*  
9 *tion, Transport in Porous Media*, **69**, 175–188.
- 10 [3] D. Aregba-Driollet, F. Diele and R. Natalini, *A Mathematical Model for the SO<sub>2</sub> Aggression*  
11 *to Calcium Carbonate Stones: Numerical Approximation and Asymptotic Analysis, SIAM*  
12 *J. APPL. MATH.* , **64** (2004), 1636–1667.
- 13 [4] Beven, K. and Feyen, J. (2002), *The Future of Distributed Modelling*. Hydrol. Process., 16:  
14 169172. doi:10.1002/hyp.325.
- 15 [5] M. Böhm, J. Devinny, F. Jahani, G. Rosen, (1998), *On a moving-boundary system modelling*  
16 *corrosion in sewer pipes*, Applied Mathematics and Computation, **92**: 247–269.
- 17 [6] M. Bohm, J. S. Devinny, F. Jahani, F. B. Mansfeld, I. G. Rosen, C. Wang, (1999), *A Moving*  
18 *Boundary Diffusion Model for the Corrosion of Concrete Wastewater Systems: Simulation*  
19 *and Experimental Validation*, Proceedings of the American Control Conference San Diego,  
20 California, June 1999: 1739–1743.
- 21 [7] F. Clareli, A. Fasano and R. Natalini, (2008), *Mathematics and monument conservation :*  
22 *Free boundary models of marble sulfation*, SIAM Journal on Applied Mathematics, **69**,  
23 No. 1. 149–168.
- 24 [8] A. Fasano, R. Natalini, (2006) *Lost Beauties of the Acropolis : What Mathematics Can Say*,  
25 SIAM News, **39**, July/August 2006.
- 26 [9] T. Fatima, N. Arab, E. P. Zemskov, A. Muntean, (2011) *Homogenization of a reaction - dif-*  
27 *fusion system modeling sulfate corrosion of concrete in locally periodic perforated domains*,  
28 Journal of Engineering Mathematics, **39**, Issue 2-3, pp 261–276.
- 29 [10] T. Fatima, A. Muntean, (2013) *Sulfate attack in sewer pipes: Derivation of a concrete*  
30 *corrosion model via two-scale convergence* Nonlinear Analysis: Real World Applications,  
31 DOI:10.1016/j.nonrwa.2012.01.019,2013.
- 32 [11] S. J. Gregg, K. S. W. Sing, (2013) *Adsorption, Surface Area and Porosity* Academic Press,  
33 (1982).
- 34 [12] F. R. Guarguaglini and R. Natalini, (2007) *Fast reaction limit and large time behavior of so-*  
35 *lutions to a nonlinear model of sulphation phenomena, Commun. Partial Differ. Equations*,  
36 **32**, 163–189.
- 37 [13] F. R. Guarguaglini and R. Natalini, (2005) *Global existence of solutions to a nonlinear model*  
38 *of sulphation phenomena in calcium carbonate stones, Nonlinear Analysis: Real World*  
39 *Applications*, **6**, 477–494.
- 40 [14] E. J. Hinch, (1991) *Perturbation Methods*, Cambridge University Press.
- 41 [15] S. Howison, A.A. Lacey, Movack, J. Ockendon, (2003) *Applied PDE's*, Oxford University  
42 Press.
- 43 [16] A. Jaklic, A. Leonardis and F. Solina, (2000) *Segmentation and Recovery of Superquadrics*,  
44 Computational imaging and vision, Vol. 20, Kluwer, Dordrecht.
- 45 [17] A.A Lacey, L.A. Herraiz, (2002), *Macroscopic models for melting derived from averaging*  
46 *microscopic Stefan problems I: Simple geometries with kinetic undercooling or surface*  
47 *tension* . Euro. Jnl. of Applied Mathematics, **11**: 153–169.
- 48 [18] A.A Lacey, L.A. Herraiz, (2002), *Macroscopic models for melting derived from averaging*  
49 *microscopic Stefan problems II: Effect of varying geometry and composition*. Euro. Jnl. of  
50 Applied Mathematics, **13**: 261–282.

- 1 [19] P. Maragos, M.A. Butt, (2000) *Curve evolution, differential morphology, and distance trans-*  
2 *forms applied to multiscale and eikonal problems*, Fundamenta Informatica, **41**, 91–129.
- 3 [20] A. Muntean, M. Böhm, (2009), *A moving-boundary problem for concrete carbonation: global*  
4 *existence and uniqueness of weak solutions*. J. Math. Anal. Appl. **350**, no. 1: 234–251.
- 5 [21] A.Muntean,V.Chalupecky, (2011) *Homogenization Method and Multiscale Modeling*, Lecture  
6 Notes of the Institute for Mathematics for Industry, vol.**34**, Kyushu University,Fukuoka,  
7 Japan.
- 8 [22] C. V. Nikolopoulos, (2010) *A Mushy Region in Concrete Corrosion* Applied Mathematical  
9 Modelling, **34**: 4012–4030.
- 10 [23] C. V. Nikolopoulos, (2015) *Macroscopic Models for A Mushy Region in Concrete Corrosion*,  
11 J. Engrg. Math. **91**, 143-163 .
- 12 [24] C. V. Nikolopoulos, (2014) *Mathematical Modelling of a Mushy Region Formation During*  
13 *Sulfation of Calcium Carbonate*, Netw. Heterog. Media **9**, (2014), no. 4, 635-654.
- 14 [25] S. Osher, J.A. Sethian (1988) *Fronts propagating with curvature-dependent speed: algorithms*  
15 *based on Hamilton-Jacobi formulations*, Journal of computational physics, **79**(1), 12–49.
- 16 [26] P.O. Persson, G. Strang (1988) *A Simple Mesh Generator in MATLAB* , SIAM Review,  
17 **46**(2), 329–345.
- 18 [27] Schröder J. (2014) A numerical two-scale homogenization scheme: the FE2-method. In:  
19 Schröder J., Hackl K. (eds) Plasticity and Beyond. CISM International Centre for Me-  
20 chanical Sciences, vol 550. Springer, Vienna